Secure NOMA Based Two-Way Relay Networks Using Artificial Noise and Full Duplex

Beixiong Zheng, Miaowen Wen, *Senior Member, IEEE*, Cheng-Xiang Wang, *Fellow, IEEE*, Xiaodong Wang, *Fellow, IEEE*, Fangjiong Chen, *Member, IEEE*, Jie Tang, *Senior Member, IEEE*, and Fei Ji, *Member, IEEE*

***Abstract*— In this paper, we develop a non-orthogonal multiple access (NOMA)-based two-way relay network with secrecy considerations, in which two users wish to exchange their NOMA signals via a trusted relay in the presence of single and multiple eavesdroppers. To ensure secure communications, the relay not only forwards confidential information to the legitimate users but also keeps emitting jamming signals all the time to degrade the performance of any potential eavesdropper. Moreover, we equip the relay and each user with the full-duplex technique in the multiple-access phase to combat the eavesdropping and improve the data transmission efficiency, respectively. We propose different decoding schemes based on the successive interference cancellation for the legitimate users, relay, and eavesdroppers. Closed-form expressions for the achievable ergodic secrecy rates of all data symbols under both single- and multiple-eavesdropper cases are derived, validated by the excellent fitting to the computer simulation results for our proposed network.**

***Index Terms*— Physical layer security, non-orthogonal multiple access (NOMA), two-way relay networks, full-duplex, artificial noise.**

I. Introduction

DUE to the continuous growth of mobile devices and rapid development of Internet of things (IoT), the fifth generation (5G) wireless communication networks impose an explosive demand on low latency and massive connectivity over limited radio resources. Non-orthogonal multiple access (NOMA), which has shown the potential to improve spectral efficiency, balance user fairness, enlarge connections, and reduce access latency, has been envisioned as a promising technology for 5G networks [1]–[3]. In contrast to the conventional orthogonal multiple access (OMA), NOMA simultaneously serves a multitude of users with the same radio resource via superposition coding, where different users are distinguished with different power levels and the successive interference cancellation (SIC) is applied to cancel the multi-user interference.

Owing to various advantages it promises, NOMA has received considerable interest in both industry and academia. The system-level performance of both uplink and downlink NOMA was studied in [4]–[6], showing better performance than conventional OMA. In [7], the performance of NOMA was studied in a cellular scenario with randomly roaming users. Under the statistical and instantaneous channel state information (CSI), the power allocation problem for NOMA to achieve the max-min fairness among users was solved in [8]. In addition, the combination of NOMA transmission with other techniques, e.g., multiple-input multiple-output (MIMO) [9]–[11], cognitive radio [12]–[14], and cooperative relaying [15]–[18], has also been investigated.

The support of massive connectivity makes the mobile user easy to access, which unfortunately also makes it easy to be wiretapped by eavesdroppers due to the broadcast nature of wireless medium. Moreover, with ever-increasing amount of sensitive data, security issues of wireless communications become more and more prominent and emergent. To ensure transmission security, the concept of physical layer (PHY) security, which was initially introduced by Wyner from the information-theoretical perspective [19], has attracted increasing attention in various wireless communication scenarios [20]–[38]. Particularly, multi-antenna techniques have extensively been studied as an efficient way to achieve security enhancements. When the eavesdropper's CSI is available at the transmitter, the secrecy capacities were investigated and analyzed under various antenna configurations and channel conditions [23]–[27]. However, in practical systems, a eavesdropper usually works in a passive way and its instantaneous CSI is unavailable to the transmitter, especially under fading channels. When the potential eavesdropper may have better channel condition and its CSI is completely unknown, one of the effective solutions called artificial noise scheme in [28] can be applied for secure transmissions, in which the information-bearing signals and the artificial noises were simultaneously transmitted to deteriorate the received signal of the potential

Manuscript received September 13, 2017; revised January 27, 2018; accepted February 16, 2018. Date of publication April 9, 2018; date of current version October 18, 2018. This work was supported in part by the National Natural Science Foundation of China under Grant U1701265, Grant 61431005, and Grant 61671211, in part by the Natural Science Foundation of Guangdong Province under Grant 2016A030308006 and Grant 2016A030311024, and in part by the Pearl River Nova Program of Guangzhou under Grant 201806010171. The work of C.-X. Wang was supported in part by the EU H2020 RISE TESTBED Project under Grant 734325, in part by the EU FP7 QUICK Project under Grant PIRSES-GA-2013-612652, and in part by the EPSRC TOUCAN Project under Grant EP/L020009/1. *(Corresponding author: Miaowen Wen.)*

B. Zheng, M. Wen, F. Chen, J. Tang, and F. Ji are with the School of Electronic and Information Engineering, South China University of Technology, Guangzhou 510641, China (email: zheng.bx@mail.scut.edu.cn; eemwwen@scut.edu.cn; eefjchen@scut.edu.cn; eejtang@scut.edu.cn; eefeiji@scut.edu.cn).

C.-X. Wang is with the Institute of Sensors, Signals and Systems, School of Engineering and Physical Sciences, Heriot-Watt University, Edinburgh EH14 4AS, U.K. (e-mail: cheng-xiang.wang@hw.ac.uk).

X. Wang is with the Department of Electrical Engineering, Columbia University, New York, NY 10027 USA (e-mail: wangx@ee.columbia.edu).

Color versions of one or more of the figures in this paper are available online at http://ieeexplore.ieee.org.

Digital Object Identifier 10.1109/JSAC.2018.2824624

eavesdroppers without impairing the legitimate users. After that, the design and analysis of artificial-noise-aided transmissions were studied in various wiretap channels, e.g., MIMO channels [29]–[32], cooperative relay channels [33]–[35], and two-way relay channels [36]–[38].

Although NOMA shows to achieve higher spectral efficiency and better user fairness than conventional OMA, the technology itself does not prevent from the information leakage and is also vulnerable to the eavesdropping. Therefore, the design of secrecy transmission for NOMA protocol is an important research topic. Unfortunately, to the best of our knowledge, the secrecy issue of NOMA has rarely been reported in the literature, except for the very recent studies [39]–[45]. The secrecy performance of NOMA in large-scale networks was analyzed in [39] and [40], where randomly deployed users and eavesdroppers were assumed. In [41], the secure problem of preventing multicast receivers from intercepting unicasting messages was investigated. The optimization problem with different designable parameters was solved in [42] under the secrecy considerations for NOMA systems. The optimization problem in terms of the secrecy sum rate was solved for the single-input single-output (SISO), multi-input single-output (MISO), and MIMO NOMA systems in [43], [44], and [45], respectively.

In this paper, we focus on the NOMA-based two-way relaying communication scenario with one pair of user nodes, one relay node, and multiple passive eavesdroppers. Two user nodes wish to exchange information via the trusted relay node in two phases: the multiple-access phase and broadcast phase. It is worth pointing out that without any protection, such relay-aided transmissions can be more vulnerable to eavesdropping because the confidential information is broadcast twice, i.e., by the users and relay. To increase the system throughput and reduce the information leakage, we propose a secure NOMA-based two-way relay network, in which the relay not only protects the network from eavesdropping but also improves the spectral efficiency by creating the heterogeneous channel condition for the NOMA users. The main contributions of this work are summarized as follows.

- In the proposed secure NOMA-based two-way relay network, we equip the relay and each user with the full-duplex technique in the multiple-access phase to combat the eavesdropping and improve the data transmission efficiency, respectively. Specifically, without requiring any extra bandwidth resource, two legitimate users receive the NOMA signals from each other under the protection of the full-duplex relay to ensure secure information exchange.
- We design different decoding schemes based on the SIC for the legitimate users, relay, and eavesdroppers, which exploit channel gain differences to achieve better decoding performance with NOMA proposal. Moreover, to consider a harsh secure scenario, we provide the eavesdroppers with a sophisticated strategy by jointly processing the signals received in the two phase to better wiretap the information.
- We analyze the performance of the secure NOMA-based two-way relay network in terms of instantaneous and ergodic secrecy rates for each data symbol. Under the assumption of independent Rayleigh fading channels, we first derive the closed-form expressions on the ergodic secrecy rates for the single-eavesdropper case. By extending the single-eavesdropper case to the multiple-eavesdropper case, we further derive the closed-form expressions on the ergodic secrecy rates under both non-colluding and colluding eavesdroppers. These closed-form expressions are in perfect agreement with simulation results.

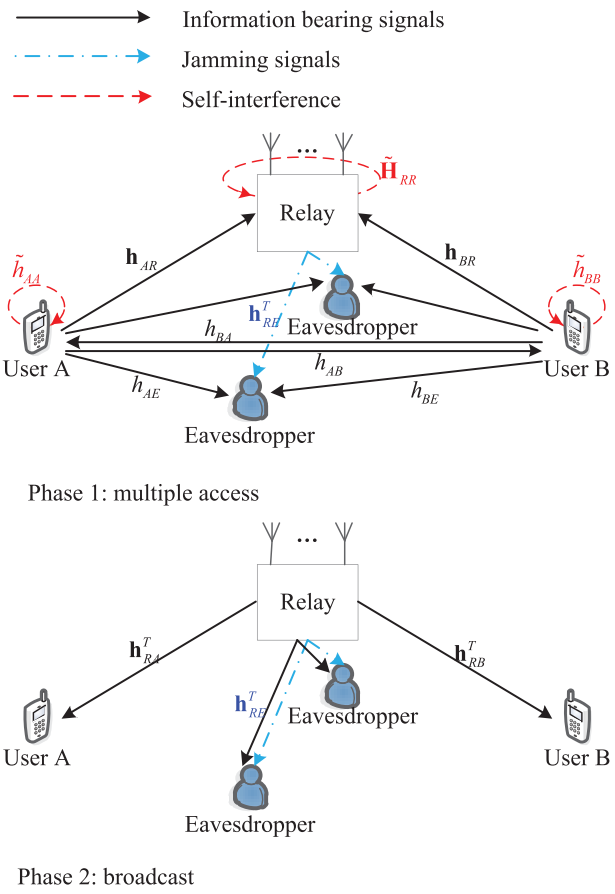

Fig. 1. An illustration of the secrecy NOMA-based TWR network.

The remainder of this paper is organized as follows. Section II describes the proposed secure NOMA-based two-way relay network and the decoding strategies. In Section III, we conduct the performance analysis of the network under the single-eavesdropper case. The secure performance of the network under multiple eavesdroppers is analyzed in Section IV. Section V presents numerical results. Finally, conclusions are drawn in Section VI.

II. Network Model and Decoding Scheme

A. Network Model

Let us consider a wireless network as shown in Fig. 1, in which one pair of user nodes (denoted by A and B) wish to exchange information via a relay node (denoted by R), under the existence of eavesdroppers (denoted by E). The relay is equipped with N_R antennas while all the other nodes only have one antenna each due to the size limitation. The eavesdroppers

are assumed to be passive all the time and attempt to intercept the information exchanged between the two legitimate users. We assume all the links are available and all the channels are flat fading and quasi-static. Without loss of generality, we first consider the case with only one eavesdropper in this section. The more general case with multiple eavesdroppers using different cooperative strategies to wiretap the information will be discussed and analyzed later in the following sections. As shown in Fig. 1, the channel gains of $A \to B$, $B \to A$, $A \to E$, and $B \to E$ are denoted by h_{AB}, h_{BA}, h_{AE}, and h_{BE}, respectively. With multiple antennas equipped at the relay, the channel gains of $A \to R$, $B \to R$, $R \to A$, $R \to B$, and $R \to E$ are denoted by $\mathbf{h}_{AR}$, $\mathbf{h}_{BR}$, $\mathbf{h}_{RA}^T$, $\mathbf{h}_{RB}^T$, and $\mathbf{h}_{RE}^T$, respectively. Moreover, it is assumed that the eavesdropper has full access to the global CSI; however, the legitimate users and relay only know that the CSI is not related to the eavesdroppers. The bidirectional communication consists of a multiple-access phase and a broadcast phase, in which the eavesdropper can overhear the signals from both phases.

1) Multiple-Access Phase: In the first phase, two legitimate users transmit their signals simultaneously to each other and the relay node while the eavesdropper receives the signals silently. For the implementation of NOMA, User A splits itself into two sub-users, say $A1$ and $A2$, with the power ratios α and $1-\alpha$ respectively, and so does User B. Then each legitimate user transmits the signals of two sub-users by adopting the superposition code, which are given in the form of

$$x_A = \sqrt{\alpha P_A} s_{A1} + \sqrt{(1-\alpha) P_A} s_{A2} \tag{1}$$

$$x_B = \sqrt{\alpha P_B} s_{B1} + \sqrt{(1-\alpha) P_B} s_{B2} \tag{2}$$

for Users A and B, respectively, where s_δ denotes the independent data symbol of Sub-user δ with $\mathbb{E}\left[|s_\delta|^2\right] = 1$ for $\delta \in \{A1, A2, B1, B2\}$, and P_A and P_B stand for the transmit powers of Users A and B, respectively. According to the NOMA principle, s_{A1} and s_{B1} are allocated with more power and we have $\sqrt{\alpha} > \sqrt{1-\alpha}$, i.e., $0.5 < \alpha < 1$. By applying (1) and (2) at user nodes, we provide receivers with the freedom to decide which fraction of the interference to decode along with the desired signal and improve the spectral efficiency by exploiting channel gain differences between sub-users.

To protect the information in the first phase, we assume the relay operates in the full-duplex mode to receive signals from the legitimate users while radiating jamming signals simultaneously to degrade the quality of the potential eavesdroppers by using the artificial noise scheme. The key idea of generating artificial noises for secure communications is to confuse the potential eavesdroppers without interfering the legitimate users by exploiting the null space of the legitimate channels. Let the singular value decomposition [46] of $\mathbf{H}_{RU} = [\mathbf{h}_{RA}\ \mathbf{h}_{RB}]^T \in \mathbb{C}^{2\times N_R}$ be expressed as

$$\mathbf{H}_{RU} = \mathbf{U}\left[\mathbf{\Lambda}\ \ \mathbf{0}_{2\times(N_R-2)}\right][\mathbf{W}_U\ \mathbf{W}_E]^H \tag{3}$$

where $\mathbf{h}_{RA} \sim \mathcal{N}_c(\mathbf{0}_{N_R\times 1}, \beta_{RA}\mathbf{I}_{N_R})$ and $\mathbf{h}_{RB} \sim \mathcal{N}_c(\mathbf{0}_{N_R\times 1}, \beta_{RB}\mathbf{I}_{N_R})$ denote the channel vectors from the relay to the legitimate users, $\mathbf{W} = [\mathbf{W}_U\ \mathbf{W}_E]$ forms an orthonormal basis of $\mathbb{C}^{N_R\times N_R}$ with $\mathbf{W}_U \in \mathbb{C}^{N_R\times 2}$ and $\mathbf{W}_E \in \mathbb{C}^{N_R\times(N_R-2)}$ standing for the range space and null space of $\mathbf{H}_{RU}$, respectively, and $\mathbf{\Lambda}$ is a diagonal matrix whose diagonal entries are two singular values. Using the artificial noise scheme, the jamming signal vector radiated at the relay in the first phase is designed in the form of

$$\mathbf{x}_R^{(1)} = \mathbf{W}_E\sqrt{\frac{P_R}{N_R-2}}\mathbf{v}^{(1)} \tag{4}$$

where $\mathbf{v}^{(1)} \sim \mathcal{N}_c(\mathbf{0}_{(N_R-2)\times 1}, \mathbf{I}_{N_R-2})$ is the artificial noise vector and P_R denotes the transmit power of the relay that is equally allocated to the N_R-2 entries of $\mathbf{v}^{(1)}$.

After suppressing the self-interference, the signal received at the relay node in the first phase can be written as

$$\begin{aligned}\mathbf{y}_R &= \mathbf{h}_{AR}x_A + \mathbf{h}_{BR}x_B + \tilde{\mathbf{H}}_{RR}\mathbf{x}_R^{(1)} + \mathbf{n}_R \\ &= \mathbf{H}_{UR}\begin{bmatrix}x_A\\ x_B\end{bmatrix} + \tilde{\mathbf{n}}_R\end{aligned} \tag{5}$$

where $\mathbf{H}_{UR} = [\mathbf{h}_{AR}\ \mathbf{h}_{BR}] \in \mathbb{C}^{N_R\times 2}$ represents the channel matrix from the legitimate users to the relay with $\mathbf{h}_{AR} \sim \mathcal{N}_c(\mathbf{0}_{N_R\times 1}, \beta_{AR}\mathbf{I}_{N_R})$ and $\mathbf{h}_{BR} \sim \mathcal{N}_c(\mathbf{0}_{N_R\times 1}, \beta_{BR}\mathbf{I}_{N_R})$, $\mathbf{n}_R \sim \mathcal{N}_c(\mathbf{0}_{N_R\times 1}, \sigma_R^2\mathbf{I}_{N_R})$ is an additive white Gaussian noise (AWGN) vector, $\tilde{\mathbf{H}}_{RR}$ denotes the residual self-interference channel due to the imperfect interference mitigation at the relay node whose entries are independent and identically distributed (i.i.d.) zero-mean complex Gaussian variables with variance β_{RR}, $\tilde{\mathbf{n}}_R = \tilde{\mathbf{H}}_{RR}\mathbf{x}_R^{(1)} + \mathbf{n}_R$ stands for the residual-interference-plus-noise vector, which is modeled by a zero-mean complex Gaussian random vector, i.e., $\tilde{\mathbf{n}}_R \sim \mathcal{N}_c(\mathbf{0}_{N_R\times 1}, \left(P_R\beta_{RR} + \sigma_R^2\right)\mathbf{I}_{N_R})$. After receiving the signals from the users as in (5), the relay first applies the zero-forcing (ZF) equalization to decompose the data streams from the two users, which can be expressed as

$$\begin{aligned}\mathbf{z}_R &= \mathbf{C}_{\mathrm{ZF}}\mathbf{y}_R = \begin{bmatrix}x_A\\ x_B\end{bmatrix} + \mathbf{C}_{\mathrm{ZF}}\tilde{\mathbf{n}}_R \\ &= \begin{bmatrix}\sqrt{\alpha P_A}s_{A1} + \sqrt{(1-\alpha)P_A}s_{A2}\\ \sqrt{\alpha P_B}s_{B1} + \sqrt{(1-\alpha)P_B}s_{B2}\end{bmatrix} + \begin{bmatrix}\bar{n}_A\\ \bar{n}_B\end{bmatrix}\end{aligned} \tag{6}$$

where $\mathbf{C}_{\mathrm{ZF}} = \left(\mathbf{H}_{UR}^H\mathbf{H}_{UR}\right)^{-1}\mathbf{H}_{UR}^H$ denotes the equalization matrix, and $\bar{n}_A$ and $\bar{n}_B$ are the equalized noises corresponding to the data streams from Users A and B, respectively. In particular, the variances of $\bar{n}_A$ and $\bar{n}_B$ are given by

$$\bar{\sigma}_A^2 = \left(P_R\beta_{RR} + \sigma_R^2\right)\left[\left(\mathbf{H}_{UR}^H\mathbf{H}_{UR}\right)^{-1}\right]_{1,1} \tag{7}$$

$$\bar{\sigma}_B^2 = \left(P_R\beta_{RR} + \sigma_R^2\right)\left[\left(\mathbf{H}_{UR}^H\mathbf{H}_{UR}\right)^{-1}\right]_{2,2} \tag{8}$$

where $[\cdot]_{i,i}$ denotes the i-th diagonal element of the square matrix. By denoting

$$\rho_A = \frac{1}{\beta_{AR}\left[\left(\mathbf{H}_{UR}^H\mathbf{H}_{UR}\right)^{-1}\right]_{1,1}},$$

$$\rho_B = \frac{1}{\beta_{BR}\left[\left(\mathbf{H}_{UR}^H\mathbf{H}_{UR}\right)^{-1}\right]_{2,2}}$$

we have $\bar{\sigma}_A^2 = \left(P_R\beta_{RR} + \sigma_R^2\right)/\left(\beta_{AR}\rho_A\right)$ and $\bar{\sigma}_B^2 = \left(P_R\beta_{RR} + \sigma_R^2\right)/\left(\beta_{BR}\rho_B\right)$, where $\rho_\delta \sim \chi^2_{2(N_R-1)}$ with the

complementary cumulative density function (CCDF) [47], [48] as

$$\bar{F}_{\rho_\delta}(x) = \exp(-x) \sum_{k=0}^{N_R-2} \frac{x^k}{k!}, \quad x \geq 0 \tag{9}$$

for $\delta \in \{A, B\}$.

Thanks to the recent advances in full-duplex mobile device [49]–[51], we also equip two legitimate user nodes with the full-duplex mode during the first phase so that they can receive the NOMA signals from each other to improve the network performance. As the artificial noise vector $\mathbf{v}^{(1)}$ is projected into the null space of $\mathbf{H}_{RU}$ in (4), the signals received at the legitimate user nodes A and B are respectively given by

$$\begin{aligned} y_A^{(1)} &= h_{BA}x_B + \tilde{h}_{AA}x_A + n_A^{(1)} \\ &= h_{BA}\left(\sqrt{\alpha P_B}s_{B1} + \sqrt{(1-\alpha)P_B}s_{B2}\right) + \tilde{n}_A^{(1)} \end{aligned} \tag{10}$$

$$\begin{aligned} y_B^{(1)} &= h_{AB}x_A + \tilde{h}_{BB}x_B + n_B^{(1)} \\ &= h_{AB}\left(\sqrt{\alpha P_A}s_{A1} + \sqrt{(1-\alpha)P_A}s_{A2}\right) + \tilde{n}_B^{(1)} \end{aligned} \tag{11}$$

which are not interfered by the jamming signal vector $\mathbf{x}_R^{(1)}$ with the leverage of the null space property $\mathbf{H}_{RU}\mathbf{W}_E = \mathbf{0}_{2\times(N_R-2)}$, where $h_{BA} \sim \mathcal{N}_c(0, \beta_{BA})$ and $h_{AB} \sim \mathcal{N}_c(0, \beta_{AB})$ are the direct links between the users, $n_A^{(1)} \sim \mathcal{N}_c(0, \sigma_A^2)$ and $n_B^{(1)} \sim \mathcal{N}_c(0, \sigma_B^2)$ are the complex AWGNs, $\tilde{h}_{AA}$ and $\tilde{h}_{BB}$ denote the residual self-interference channels with the normalized gains β_{AA} and β_{BB}, respectively, and $\tilde{n}_A^{(1)} = \tilde{h}_{AA}x_A + n_A^{(1)}$ and $\tilde{n}_B^{(1)} = \tilde{h}_{BB}x_B + n_B^{(1)}$ stand for the residual-interference-plus-noises, which are modeled by the zero-mean complex Gaussian random variables, i.e., $\tilde{n}_A^{(1)} \sim \mathcal{N}_c(0, P_A\beta_{AA} + \sigma_A^2)$ and $\tilde{n}_B^{(1)} \sim \mathcal{N}_c(0, P_B\beta_{BB} + \sigma_B^2)$ at Users A and B, respectively.

Concurrently, the signal received at the passive eavesdropper in the first phase is given by

$$\begin{aligned} y_E^{(1)} &= h_{AE}x_A + h_{BE}x_B + \mathbf{h}_{RE}^T\mathbf{x}_R^{(1)} + n_E^{(1)} \\ &= h_{AE}\left(\sqrt{\alpha P_A}s_{A1} + \sqrt{(1-\alpha)P_A}s_{A2}\right) \\ &\quad + h_{BE}\left(\sqrt{\alpha P_B}s_{B1} + \sqrt{(1-\alpha)P_B}s_{B2}\right) \\ &\quad + \mathbf{h}_{RE}^T\mathbf{W}_E\sqrt{\frac{P_R}{N_R-2}}\mathbf{v}^{(1)} + n_E^{(1)} \end{aligned} \tag{12}$$

where $h_{AE} \sim \mathcal{N}_c(0, \beta_{AE})$, $h_{BE} \sim \mathcal{N}_c(0, \beta_{BE})$, $\mathbf{h}_{RE} \sim \mathcal{N}_c(\mathbf{0}_{N_R\times 1}, \beta_{RE}\mathbf{I}_{N_R})$ are the channels related to the eavesdropper, and $n_E^{(1)} \sim \mathcal{N}_c(0, \sigma_E^2)$ is the complex AWGN.

2) Broadcast Phase: After decoupling the two data streams by ZF equalization, the relay decodes them separately according to (6). Then, to confuse the potential eavesdropper and coordinate the transmission of two low-power sub-users ($A2$ and $B2$) simultaneously in the second phase, the relay mixes some artificial noises with two data symbols s_{A2} and s_{B2}, which is designed in the form of

$$\mathbf{x}_R^{(2)} = \mathbf{W}_U\sqrt{\frac{\phi P_R}{2}}\begin{bmatrix} s_{B2} \\ s_{A2} \end{bmatrix} + \mathbf{W}_E\sqrt{\frac{(1-\phi)P_R}{N_R-2}}\mathbf{v}^{(2)} \tag{13}$$

where ϕ denotes the power allocation ratio of the signal power to the total transmit power P_R for the artificial noise scheme and $\mathbf{v}^{(2)} \sim \mathcal{N}_c(\mathbf{0}_{(N_R-2)\times 1}, \mathbf{I}_{N_R-2})$ is the artificial noise vector generated in the second phase.

As the artificial noise vector $\mathbf{v}^{(2)}$ is projected into the null space of $\mathbf{H}_{UR}$ in (13), the signals received at the legitimate user nodes A and B are respectively given by

$$y_A^{(2)} = \mathbf{h}_{RA}^T\mathbf{x}_R^{(2)} + n_A^{(2)} = \mathbf{h}_{RA}^T\mathbf{W}_U\sqrt{\frac{\phi P_R}{2}}\begin{bmatrix} s_{B2} \\ s_{A2} \end{bmatrix} + n_A^{(2)} \tag{14}$$

$$y_B^{(2)} = \mathbf{h}_{RB}^T\mathbf{x}_R^{(2)} + n_B^{(2)} = \mathbf{h}_{RB}^T\mathbf{W}_U\sqrt{\frac{\phi P_R}{2}}\begin{bmatrix} s_{B2} \\ s_{A2} \end{bmatrix} + n_B^{(2)} \tag{15}$$

where $\mathbf{h}_{RA} \sim \mathcal{N}_c(\mathbf{0}_{N_R\times 1}, \beta_{RA}\mathbf{I}_{N_R})$ and $\mathbf{h}_{RB} \sim \mathcal{N}_c(\mathbf{0}_{N_R\times 1}, \beta_{RB}\mathbf{I}_{N_R})$ denote the channels from the relay to the users, and $n_A^{(2)} \sim \mathcal{N}_c(0, \sigma_A^2)$ and $n_B^{(2)} \sim \mathcal{N}_c(0, \sigma_B^2)$ are the complex AWGNs at Users A and B, respectively. Since signal s_{A2} is generated by User A, User A can perform the self-interference cancellation of s_{A2} before decoding its desired signal s_{B2} in (14), and so can User B in (15). By denoting $\mathbf{W}_U = [\mathbf{w}_A\ \mathbf{w}_B]$, we can rewrite the signal models in (14) and (15) after the self-interference cancellation as

$$y_A^{(2)} = \mathbf{h}_{RA}^T\mathbf{w}_A\sqrt{\frac{\phi P_R}{2}}s_{B2} + n_A^{(2)} \tag{16}$$

$$y_B^{(2)} = \mathbf{h}_{RB}^T\mathbf{w}_B\sqrt{\frac{\phi P_R}{2}}s_{A2} + n_B^{(2)}. \tag{17}$$

During the second phase, the signal received at the eavesdropper is given by

$$\begin{aligned} y_E^{(2)} &= \mathbf{h}_{RE}^T\mathbf{x}_R^{(2)} + n_E^{(2)} = \mathbf{h}_{RE}^T\mathbf{w}_B\sqrt{\frac{\phi P_R}{2}}s_{A2} + \mathbf{h}_{RE}^T\mathbf{w}_A \\ &\quad \times\sqrt{\frac{\phi P_R}{2}}s_{B2} + \mathbf{h}_{RE}^T\mathbf{W}_E\sqrt{\frac{(1-\phi)P_R}{N_R-2}}\mathbf{v}^{(2)} + n_E^{(2)} \end{aligned} \tag{18}$$

where $n_E^{(2)} \sim \mathcal{N}_c(0, \sigma_E^2)$ is the complex AWGN in the second phase.

Remark: To ensure the secure communication, the relay keeps emitting the jamming signals to degrade the performance of the potential eavesdroppers by employing the artificial noise scheme. In the first phase the relay only emits the pure jamming signals while in the second phase it transmits the mixture of the information-bearing signals and the jamming signals. In that way, the relay plays two important roles in the secure NOMA-based two-way relay network: not only forwards the confidential information for two sub-users but also jams the potential eavesdroppers.

B. Decoding Scheme Based on SIC

In (6), the relay decodes s_{A1} and s_{B1} by treating s_{A2} and s_{B2} as interference, respectively, where the signal-to-interference-plus-noise ratios (SINRs) for s_{A1} and s_{B1} are

given by

$$\gamma_{A1}^{R} = \frac{\alpha P_A}{(1-\alpha) P_A + \bar{\sigma}_A^2} = \frac{\alpha P_A}{(1-\alpha) P_A + \frac{P_R \beta_{RR} + \sigma_R^2}{\beta_{AR}\rho_A}} \quad (19)$$

$$\gamma_{B1}^{R} = \frac{\alpha P_B}{(1-\alpha) P_B + \bar{\sigma}_B^2} = \frac{\alpha P_B}{(1-\alpha) P_B + \frac{P_R \beta_{RR} + \sigma_R^2}{\beta_{BR}\rho_B}}. \quad (20)$$

After using the SIC to remove the interference of s_{A1} and s_{B1}, the relay then decodes s_{A2} and s_{B2} with the SINRs given by

$$\gamma_{A2}^{R} = \frac{(1-\alpha) P_A}{\bar{\sigma}_A^2} = \frac{(1-\alpha) P_A}{\frac{P_R \beta_{RR} + \sigma_R^2}{\beta_{AR}\rho_A}} = \frac{(1-\alpha) P_A \beta_{AR}\rho_A}{P_R \beta_{RR} + \sigma_R^2} \quad (21)$$

$$\gamma_{B2}^{R} = \frac{(1-\alpha) P_B}{\bar{\sigma}_B^2} = \frac{(1-\alpha) P_B}{\frac{P_R \beta_{RR} + \sigma_R^2}{\beta_{BR}\rho_B}} = \frac{(1-\alpha) P_B \beta_{BR}\rho_B}{P_R \beta_{RR} + \sigma_R^2}. \quad (22)$$

During the first phase, by treating s_{B2} and s_{A2} as interference, Users B and A decode s_{A1} and s_{B1} according to (11) and (10) with the SINRs given by

$$\gamma_{A1}^{B} = \frac{|h_{AB}|^2 \alpha P_A}{|h_{AB}|^2 (1-\alpha) P_A + P_B \beta_{BB} + \sigma_B^2} \quad (23)$$

$$\gamma_{B1}^{A} = \frac{|h_{BA}|^2 \alpha P_B}{|h_{BA}|^2 (1-\alpha) P_B + P_A \beta_{AA} + \sigma_A^2}. \quad (24)$$

While in the second phase, Users B and A decode s_{A2} and s_{B2} directly in (17) and (16) after the self-interference cancellation, leading to the signal-to-noise ratios (SNRs) for s_{A2} and s_{B2} given by

$$\gamma_{A2}^{B} = \frac{\left|\mathbf{h}_{RB}^T \mathbf{w}_B\right|^2 \phi P_R}{2\sigma_B^2} \quad (25)$$

$$\gamma_{B2}^{A} = \frac{\left|\mathbf{h}_{RA}^T \mathbf{w}_A\right|^2 \phi P_R}{2\sigma_A^2}. \quad (26)$$

From above, it can be observed that the decoding of different data symbols is associated with different channels, which exploits the channel gain differences to achieve better system performance with NOMA proposal.

In the proposed NOMA-based two-way relay network, the potential eavesdropper can overhear the confidential information twice, namely, the information transmitted by the legitimate users in the first phase and the information broadcast by the relay in the second phase. In the first phase, the eavesdropper receives four data symbols s_{A1}, s_{A2}, s_{B1}, and s_{B2} simultaneously, which can be tough to decode by using the SIC scheme based on (12) only. While in the second phase, the eavesdropper only receives two data symbols s_{A2} and s_{B2} according to (18), which is more feasible by using the SIC scheme. Therefore, to better wiretap the information from the perspective of the eavesdropper, we provide it with a sophisticated strategy by first decoding s_{A2} and s_{B2} in (18), and then stripping them off before decoding s_{A1} and s_{B1} in (12). Specifically, based on (18), the eavesdropper first decodes s_{A2} by treating s_{B2} as interference, yielding the SINR of s_{A2} as

$$\gamma_{A2}^{E} = \frac{\frac{\left|\mathbf{h}_{RE}^T \mathbf{w}_B\right|^2 \phi P_R}{2}}{\frac{\left|\mathbf{h}_{RE}^T \mathbf{w}_A\right|^2 \phi P_R}{2} + \frac{(1-\phi) P_R \left\|\mathbf{h}_{RE}^T \mathbf{W}_E\right\|^2}{N_R - 2} + \sigma_E^2} \quad (27)$$

then decodes s_{B2} after subtracting s_{A2}, obtaining the SINR of s_{B2} as

$$\gamma_{B2}^{E} = \frac{\frac{\left|\mathbf{h}_{RE}^T \mathbf{w}_A\right|^2 \phi P_R}{2}}{\frac{(1-\phi) P_R \left\|\mathbf{h}_{RE}^T \mathbf{W}_E\right\|^2}{N_R - 2} + \sigma_E^2}. \quad (28)$$

As the eavesdropper has decoded s_{A2} and s_{B2}, it can strip them off in (12), which yields

$$y_E^{(1)} = h_{AE}\sqrt{\alpha P_A} s_{A1} + h_{BE}\sqrt{\alpha P_B} s_{B1} + \mathbf{h}_{RE}^T \mathbf{W}_E \sqrt{\frac{P_R}{N_R - 2}} \mathbf{v}^{(1)} + n_E^{(1)}. \quad (29)$$

Based on (29), the eavesdropper first decodes s_{A1} by treating s_{B1} as interference, which obtains the SINR of s_{A1} as

$$\gamma_{A1}^{E} = \frac{|h_{AE}|^2 \alpha P_A}{|h_{BE}|^2 \alpha P_B + \frac{P_R \left\|\mathbf{h}_{RE}^T \mathbf{W}_E\right\|^2}{N_R - 2} + \sigma_E^2}. \quad (30)$$

After applying the SIC to cancel the interference of s_{A1} in (29), the eavesdropper then decodes s_{B1} with the SINR given by

$$\gamma_{B1}^{E} = \frac{|h_{BE}|^2 \alpha P_B}{\frac{P_R \left\|\mathbf{h}_{RE}^T \mathbf{W}_E\right\|^2}{N_R - 2} + \sigma_E^2}. \quad (31)$$

As revealed in (27), (28), (30), and (31), the eavesdropper first decodes the data symbols from User A and then from User B, which is a specific decoding order that we consider for the eavesdropper. It is worth pointing out different decoding orders will result in different SINRs and further different ergodic rates of data symbols achieved by the eavesdropper, which will not be discussed further due to the limited space.

III. Performance Analysis for The Single-Eavesdropper Case

In this section, we analyze the performance of the proposed network in terms of secrecy rate. Specifically, the instantaneous and ergodic secrecy rates of each data symbol are respectively given by [52]

$$C_\delta^{sec} = \left[C_\delta - C_\delta^E\right]^+, \quad \bar{C}_\delta^{sec} = \left[\bar{C}_\delta - \bar{C}_\delta^E\right]^+ \quad (32)$$

for $\delta \in \{A1, A2, B1, B2\}$ and $[x]^+ = \max\{x, 0\}$, where C_δ and $\bar{C}_\delta$ denote the instantaneous and ergodic rates of data symbol s_δ for the legitimate channel, respectively, and C_δ^E and $\bar{C}_\delta^E$ denote the instantaneous and ergodic rates of data symbol s_δ for the wiretap channel, respectively. In the following, we will derive both the instantaneous and ergodic rates for different data symbols, based on which the secrecy rates can be calculated via (32).

A. Achievable Rate Analysis for Legitimate Users

As illustrated in Section II-B, regardless of the eavesdropper, data symbols s_{A1}, s_{A2}, s_{B1}, and s_{B2} should be decoded at the legitimate users as well as the relay. To ensure the decoding correctness of s_{A1} at the relay and User B, the achievable rate of s_{A1} using (19) and (23) should be

$$\begin{aligned}C_{A1} &= \frac{1}{2}\min\left\{\log_2\left(1+\gamma_{A1}^R\right),\log_2\left(1+\gamma_{A1}^B\right)\right\}\\ &= \frac{1}{2}\log_2\left(1+\min\left\{\gamma_{A1}^R,\gamma_{A1}^B\right\}\right) = \frac{1}{2}\log_2\Bigg(1\\ &\quad+\min\left\{\frac{\alpha P_A}{(1-\alpha)P_A+\frac{P_R\beta_{RR}+\sigma_R^2}{\beta_{AR}\rho_A}},\right.\\ &\quad\left.\frac{|h_{AB}|^2\alpha P_A}{|h_{AB}|^2(1-\alpha)P_A+P_B\beta_{BB}+\sigma_B^2}\right\}\Bigg)\\ &= \frac{1}{2}\log_2\left(1+\frac{\alpha P_A\min\left\{\frac{\beta_{AR}\rho_A}{P_R\beta_{RR}+\sigma_R^2},\frac{|h_{AB}|^2}{P_B\beta_{BB}+\sigma_B^2}\right\}}{(1-\alpha)P_A\min\left\{\frac{\beta_{AR}\rho_A}{P_R\beta_{RR}+\sigma_R^2},\frac{|h_{AB}|^2}{P_B\beta_{BB}+\sigma_B^2}\right\}+1}\right)\\ &= \frac{1}{2}\log_2\left(1+P_A\min\left\{\frac{\beta_{AR}\rho_A}{P_R\beta_{RR}+\sigma_R^2},\frac{|h_{AB}|^2}{P_B\beta_{BB}+\sigma_B^2}\right\}\right)\\ &\quad-\frac{1}{2}\log_2\Bigg(1+(1-\alpha)P_A\\ &\quad\times\min\left\{\frac{\beta_{AR}\rho_A}{P_R\beta_{RR}+\sigma_R^2},\frac{|h_{AB}|^2}{P_B\beta_{BB}+\sigma_B^2}\right\}\Bigg).\end{aligned}\tag{33}$$

Following a procedure similar to (33), for symbol s_{B1} decoded at the relay and User A, its achievable rate using (20) and (24) is given by

$$\begin{aligned}C_{B1} &= \frac{1}{2}\min\left\{\log_2\left(1+\gamma_{B1}^R\right),\log_2\left(1+\gamma_{B1}^A\right)\right\}\\ &= \frac{1}{2}\log_2\left(1+P_B\min\left\{\frac{\beta_{BR}\rho_B}{P_R\beta_{RR}+\sigma_R^2},\frac{|h_{BA}|^2}{P_A\beta_{AA}+\sigma_A^2}\right\}\right)\\ &\quad-\frac{1}{2}\log_2\Bigg(1+(1-\alpha)P_B\\ &\quad\times\min\left\{\frac{\beta_{BR}\rho_B}{P_R\beta_{RR}+\sigma_R^2},\frac{|h_{BA}|^2}{P_A\beta_{AA}+\sigma_A^2}\right\}\Bigg).\end{aligned}\tag{34}$$

By using (21) and (25), the achievable rate associated with symbol s_{A2} is obtained as

$$\begin{aligned}C_{A2} &= \frac{1}{2}\min\left\{\log_2\left(1+\gamma_{A2}^R\right),\log_2\left(1+\gamma_{A2}^B\right)\right\}\\ &= \frac{1}{2}\log_2\left(1+\min\left\{\frac{(1-\alpha)P_A\beta_{AR}\rho_A}{P_R\beta_{RR}+\sigma_R^2},\right.\right.\\ &\quad\left.\left.\frac{\left|\mathbf{h}_{RB}^T\mathbf{w}_B\right|^2\phi P_R}{2\sigma_B^2}\right\}\right).\end{aligned}\tag{35}$$

Similarly, by using (22) and (26), the achievable rate of symbol s_{B2} is obtained as

$$\begin{aligned}C_{B2} &= \frac{1}{2}\min\left\{\log_2\left(1+\gamma_{B2}^R\right),\log_2\left(1+\gamma_{B2}^B\right)\right\}\\ &= \frac{1}{2}\log_2\left(1+\min\left\{\frac{(1-\alpha)P_B\beta_{BR}\rho_B}{P_R\beta_{RR}+\sigma_R^2},\right.\right.\\ &\quad\left.\left.\frac{\left|\mathbf{h}_{RA}^T\mathbf{w}_A\right|^2\phi P_R}{2\sigma_A^2}\right\}\right).\end{aligned}\tag{36}$$

Based on the above instantaneous results on achievable rates, we will derive the ergodic rates of the four data symbols for the legitimate users in the following.

Proposition 1: By defining the function

$$\begin{aligned}\mathbb{D}(k,\mu,b) &\triangleq \int_0^\infty \frac{x^k\exp(-\mu x)}{x+b}dx\\ &= -(-b)^k\exp(b\mu)\,\mathrm{Ei}(-b\mu)\\ &\quad+\sum_{n=1}^{k}(n-1)!(-b)^{k-n}\mu^{-n}\end{aligned}\tag{37}$$

in which $\mathrm{Ei}(\cdot)$ denotes the exponential integral function [53, eq. (8.211.1)], the ergodic rate of s_{A1} can be expressed as

$$\begin{aligned}\bar{C}_{A1} &= \frac{1}{2\ln 2}\sum_{k=0}^{N_R-2}\frac{\left(\frac{P_R\beta_{RR}+\sigma_R^2}{\beta_{AR}}\right)^k}{k!}\\ &\quad\times\Bigg(\mathbb{D}\Big(k,\frac{P_R\beta_{RR}+\sigma_R^2}{\beta_{AR}}+\frac{P_B\beta_{BB}+\sigma_B^2}{\beta_{AB}},\frac{1}{P_A}\Big)\\ &\quad-\mathbb{D}\left(k,\frac{P_R\beta_{RR}+\sigma_R^2}{\beta_{AR}}+\frac{P_B\beta_{BB}+\sigma_B^2}{\beta_{AB}},\frac{1}{(1-\alpha)P_A}\right)\Bigg).\end{aligned}\tag{38}$$

Proof: See Appendix A. ∎

Following the similar derivations in the proof of Proposition 1, we can obtain the ergodic rate of s_{B1} as

$$\begin{aligned}\bar{C}_{B1} &= \frac{1}{2\ln 2}\sum_{k=0}^{N_R-2}\frac{\left(\frac{P_R\beta_{RR}+\sigma_R^2}{\beta_{BR}}\right)^k}{k!}\\ &\quad\times\Bigg(\mathbb{D}\Big(k,\frac{P_R\beta_{RR}+\sigma_R^2}{\beta_{BR}}+\frac{P_A\beta_{AA}+\sigma_A^2}{\beta_{BA}},\frac{1}{P_B}\Big)\\ &\quad-\mathbb{D}\left(k,\frac{P_R\beta_{RR}+\sigma_R^2}{\beta_{BR}}+\frac{P_A\beta_{AA}+\sigma_A^2}{\beta_{BA}},\frac{1}{(1-\alpha)P_B}\right)\Bigg).\end{aligned}\tag{39}$$

Proposition 2: Given the function defined in (37), the ergodic rate of s_{A2} can be expressed as

$$\begin{aligned}\bar{C}_{A2} &= \frac{1}{2\ln 2}\sum_{k=0}^{N_R-2}\frac{\left(\frac{P_R\beta_{RR}+\sigma_R^2}{(1-\alpha)P_A\beta_{AR}}\right)^k}{k!}\\ &\quad\times\mathbb{D}\left(k,\frac{P_R\beta_{RR}+\sigma_R^2}{(1-\alpha)P_A\beta_{AR}}+\frac{2\sigma_B^2}{\phi P_R\beta_{RB}},1\right).\end{aligned}\tag{40}$$

Proof: See Appendix B. ∎

Following a similar methodology in the proof of Proposition 2, we can obtain the ergodic rate of s_{B2} as

$$\bar{C}_{B2} = \frac{1}{2\ln 2}\sum_{k=0}^{N_R-2}\frac{\left(\frac{P_R\beta_{RR}+\sigma_R^2}{(1-\alpha)P_B\beta_{BR}}\right)^k}{k!} \times\mathbb{D}\left(k, \frac{P_R\beta_{RR}+\sigma_R^2}{(1-\alpha)P_B\beta_{BR}}+\frac{2\sigma_A^2}{\phi P_R\beta_{RA}}, 1\right). \quad (41)$$

B. Achievable Rate Analysis for Eavesdropper

According to (27), (28), (30), and (31), the instantaneous achievable rate of each data symbol at the eavesdropper can be calculated via

$$C_\delta^E = \frac{1}{2}\log_2\left(1+\gamma_\delta^E\right) \quad (42)$$

for $\delta \in \{A1, A2, B1, B2\}$. Given the instantaneous results of achievable rates above, in the following we will derive the ergodic rates of the four data symbols achieved at the eavesdropper.

Proposition 3: By defining the function

$$\mathbb{G}(i,\mu,b) \triangleq \int_0^\infty \frac{\exp(-\mu x)}{(x+b)^i}dx = \frac{1}{(i-1)!}\sum_{k=1}^{i-1}(k-1)! \times(-\mu)^{i-k-1}b^{-k} - \frac{(-\mu)^{i-1}}{(i-1)!}\exp(b\mu)\,\mathrm{Ei}(-\mathrm{b}\mu) \quad (43)$$

the ergodic rate of s_{A2} at the eavesdropper can be expressed as

$$\bar{C}_{A2}^E = \frac{1}{2\ln 2}\left(\sum_{i=1}^{N_R-2}\Omega_{A2}^i\mathbb{G}\left(i, \frac{2\sigma_E^2}{\phi P_R\beta_{RE}}, \frac{\phi(N_R-2)}{2(1-\phi)}\right) + \sum_{i=1}^{2}\Psi_{A2}^i\mathbb{G}\left(i, \frac{2\sigma_E^2}{\phi P_R\beta_{RE}}, 1\right)\right) \quad (44)$$

where

$$\Omega_{A2}^i = \left(\frac{\phi(N_R-2)}{2(1-\phi)}\right)^{N_R-2}\frac{(-1)^{N_R-2-i}(N_R-1-i)}{\left(1-\frac{\phi(N_R-2)}{2(1-\phi)}\right)^{N_R-i}} \quad (45)$$

$$\Psi_{A2}^i = \left(\frac{\phi(N_R-2)}{2(1-\phi)}\right)^{N_R-2}\frac{(-1)^{2-i}(N_R-1-i)!}{(N_R-3)!\left(\frac{\phi(N_R-2)}{2(1-\phi)}-1\right)^{N_R-i}}. \quad (46)$$

Proof: See Appendix C. ∎

Following the similar derivations in the proof of the Proposition 3, we can obtain the CCDFs of γ_{B2}^E, γ_{A1}^E, and γ_{B1}^E in (28), (30), and (31) as

$$\bar{F}_{\gamma_{B2}^E} = \frac{\exp\left(-\frac{2\sigma_E^2}{\phi P_R\beta_{RE}}x\right)}{\left(1+\frac{2(1-\phi)}{\phi(N_R-2)}x\right)^{N_R-2}} \quad (47)$$

$$\bar{F}_{\gamma_{A1}^E} = \frac{\exp\left(-\frac{\sigma_E^2}{\alpha P_A\beta_{AE}}x\right)}{\left(1+\frac{P_R\beta_{RE}}{\alpha P_A\beta_{AE}(N_R-2)}x\right)^{N_R-2}(x+1)} \quad (48)$$

$$\bar{F}_{\gamma_{B1}^E} = \frac{\exp\left(-\frac{\sigma_E^2}{\alpha P_B\beta_{BE}}x\right)}{\left(1+\frac{P_R\beta_{RE}}{\alpha P_B\beta_{BE}(N_R-2)}x\right)^{N_R-2}}. \quad (49)$$

The ergodic rates of s_{B2}, s_{A1}, s_{B1} achieved by the eavesdropper are given by

$$\bar{C}_{B2}^E = \frac{1}{2\ln 2}\left(\sum_{i=1}^{N_R-2}\Omega_{B2}^i\mathbb{G}\left(i, \frac{2\sigma_E^2}{\phi P_R\beta_{RE}}, \frac{\phi(N_R-2)}{2(1-\phi)}\right) + \Psi_{B2}^1\mathbb{G}\left(1, \frac{2\sigma_E^2}{\phi P_R\beta_{RE}}, 1\right)\right) \quad (50)$$

$$\bar{C}_{A1}^E = \frac{1}{2\ln 2}\left(\sum_{i=1}^{N_R-2}\Omega_{A1}^i\mathbb{G}\left(i, \frac{\sigma_E^2}{\alpha P_A\beta_{AE}}, \frac{\alpha P_A\beta_{AE}(N_R-2)}{P_R\beta_{RE}}\right) + \sum_{i=1}^{2}\Psi_{A1}^i\mathbb{G}\left(i, \frac{\sigma_E^2}{\alpha P_A\beta_{AE}}, 1\right)\right) \quad (51)$$

$$\bar{C}_{B1}^E = \frac{1}{2\ln 2}\left(\sum_{i=1}^{N_R-2}\Omega_{B1}^i\mathbb{G}\left(i, \frac{\sigma_E^2}{\alpha P_B\beta_{BE}}, \frac{\alpha P_A\beta_{BE}(N_R-2)}{P_R\beta_{RE}}\right) + \Psi_{B1}^1\mathbb{G}\left(1, \frac{\sigma_E^2}{\alpha P_B\beta_{BE}}, 1\right)\right) \quad (52)$$

where Ω_δ^i and Ψ_δ^i for $\delta \in \{A1, B1, B2\}$ are the coefficients obtained by using the partial-fraction expansion [54, appendix], similar to (45) and (46). After we have the results for the legitimate users in (38)–(41) and for the eavesdropper in (44) and (50)–(52), the ergodic secrecy rate of each data symbol can be calculated via (32) for the proposed network under the single-eavesdropper case.

IV. Extension to Multiple Eavesdroppers

In this section, we consider the network under the existence of multiple eavesdroppers, where the number of eavesdroppers is denoted by N_E. When multiple eavesdroppers sneak into the network, their noise levels may be different and even unknown to the legitimate users and the relay. Therefore, to ensure secure communications, it is reasonable to consider the worst-case scenario where the noises are extremely small at the eavesdroppers (i.e., $\sigma_{E_i}^2 = 0$ for $i = 1, \ldots, N_E$) [28], [31], [32]. We assume each eavesdropper experiences independent channel fading and follows the same signal model as the single-eavesdropper case in Section II-A. In the following, we consider two cases, namely, non-colluding and colluding eavesdroppers.

A. Non-colluding Case

According to the SINRs of different data symbols given in (27), (28), (30), and (31) with $\sigma_E^2 = 0$ and following the similar derivations in (82), we can obtain

$$\bar{F}_{\gamma_{A1}^{E_i}} = \left(1+\frac{P_R\beta_{RE}}{\alpha P_A\beta_{AE}(N_R-2)}x\right)^{2-N_R}(x+1)^{-1} \quad (53)$$

$$\bar{F}_{\gamma_{A2}^{E_i}} = \left(1+\frac{2(1-\phi)}{\phi(N_R-2)}x\right)^{2-N_R}(x+1)^{-1} \quad (54)$$

$$\bar{F}_{\gamma_{B1}^{E_i}} = \left(1+\frac{P_R\beta_{RE}}{\alpha P_B\beta_{BE}(N_R-2)}x\right)^{2-N_R} \quad (55)$$

$$\bar{F}_{\gamma_{B2}^{E_i}} = \left(1+\frac{2(1-\phi)}{\phi(N_R-2)}x\right)^{2-N_R} \quad (56)$$

for $i = 1, \ldots, N_E$. We assume the eavesdroppers work in a non-colluding way to wiretap the information [29], [55], [56] and the highest SINR of each data symbol is chosen for decoding, i.e., $\gamma_\delta^E = \max\left\{\gamma_\delta^{E_1}, \gamma_\delta^{E_2}, \ldots, \gamma_\delta^{E_{N_E}}\right\}$, whose CDF can be obtained as

$$\begin{aligned} F_{\gamma_\delta^E}(x) &= \Pr\left\{\gamma_\delta^{E_1} < x, \gamma_\delta^{E_2} < x, \ldots, \gamma_\delta^{E_{N_E}} < x\right\} \\ &= \prod_{i=1}^{N_E} F_{\gamma_\delta^{E_i}} = \left(1 - \bar{F}_{\gamma_\delta^{E_1}}\right)^{N_E} \\ &= 1 + \sum_{i=1}^{N_E} \binom{N_E}{i} \left(-\bar{F}_{\gamma_\delta^{E_1}}\right)^i \end{aligned} \tag{57}$$

where $\delta \in \{A1, A2, B1, B2\}$ and $\binom{N_E}{i}$ denotes the binomial coefficient. With (57), the ergodic rate of each data symbol achieved by the non-colluding eavesdroppers is given by

$$\begin{aligned} \bar{C}_\delta^E &= \int_0^\infty \frac{1}{2}\log_2(1+x)\, f_{\gamma_\delta^E}(x)dx \\ &= \frac{1}{2\ln 2}\int_0^\infty \frac{1 - F_{\gamma_\delta^E}(x)}{1+x}dx \\ &= -\frac{1}{2\ln 2}\sum_{i=1}^{N_E}\binom{N_E}{i}\int_0^\infty \frac{\left(-\bar{F}_{\gamma_\delta^{E_1}}\right)^i}{1+x}dx \end{aligned} \tag{58}$$

where $\delta \in \{A1, A2, B1, B2\}$ and integration by parts is applied to (58). By substituting (53)–(56) into (58) and using [53, Eq. (3.197.5)] to the integral parts, we can obtain

$$\begin{aligned} \bar{C}_{A1}^E = &\frac{1}{2\ln 2}\sum_{i=1}^{N_E}\binom{N_E}{i}(-1)^i \mathrm{B}\left(1, (N_R-1)\, i\right) \\ &{}_2F_1\Big(\left(N_R-2\right) i, 1; \left(N_R-1\right) i + 1; 1 \\ &- \frac{P_R\beta_{RE}}{\alpha P_A \beta_{AE}\left(N_R-2\right)}\Big) \end{aligned} \tag{59}$$

$$\begin{aligned} \bar{C}_{A2}^E = &\frac{1}{2\ln 2}\sum_{i=1}^{N_E}\binom{N_E}{i}(-1)^i \mathrm{B}\left(1, (N_R-1)\, i\right) \\ &{}_2F_1\Big(\left(N_R-2\right) i, 1; \left(N_R-1\right) i + 1; 1 - \frac{2\left(1-\phi\right)}{\phi\left(N_R-2\right)}\Big) \end{aligned} \tag{60}$$

$$\begin{aligned} \bar{C}_{B1}^E = &\frac{1}{2\ln 2}\sum_{i=1}^{N_E}\binom{N_E}{i}(-1)^i \mathrm{B}\left(1, (N_R-2)\, i\right) \\ &{}_2F_1\Big(\left(N_R-2\right) i, 1; \left(N_R-2\right) i + 1; 1 \\ &- \frac{P_R\beta_{RE}}{\alpha P_A \beta_{AE}\left(N_R-2\right)}\Big) \end{aligned} \tag{61}$$

$$\begin{aligned} \bar{C}_{B2}^E = &\frac{1}{2\ln 2}\sum_{i=1}^{N_E}\binom{N_E}{i}(-1)^i \mathrm{B}\left(1, (N_R-2)\, i\right) \\ &{}_2F_1\Big(\left(N_R-2\right) i, 1; \left(N_R-2\right) i + 1; 1 - \frac{2\left(1-\phi\right)}{\phi\left(N_R-2\right)}\Big) \end{aligned} \tag{62}$$

where $\mathrm{B}(x, y)$ is the Beta function [53, Sec. 8.38], and ${}_2F_1(\alpha, \beta; \gamma; z)$ is the Gauss hypergeometric function and its transformation formulas can be referred to [53, Sec. 9.10-9.13]. With the results for the legitimate users in (38)–(41) and for the non-colluding eavesdroppers in (59)–(62), the ergodic secrecy rate of each data symbol can be finally obtained via (32).

B. Colluding Case

Next, we study the case under multiple colluding eavesdroppers, where $N_R \geq N_E + 2$ to guarantee secure communications [31]. By extending the signal model of single-eavesdropper in (18) and (29) to the noiseless case with multiple colluding eavesdroppers, we have

$$\begin{aligned} \mathbf{y}_E^{(1)} = &\mathbf{h}_{AE}\sqrt{\alpha P_A}s_{A1} + \mathbf{h}_{BE}\sqrt{\alpha P_B}s_{B1} \\ &+ \mathbf{H}_{RE}^T\mathbf{W}_E\sqrt{\frac{P_R}{N_R-2}}\mathbf{v}^{(1)} \end{aligned} \tag{63}$$

$$\begin{aligned} \mathbf{y}_E^{(2)} = &\mathbf{H}_{RE}^T\mathbf{w}_B\sqrt{\frac{\phi P_R}{2}}s_{A2} + \mathbf{H}_{RE}^T\mathbf{w}_A\sqrt{\frac{\phi P_R}{2}}s_{B2} \\ &+ \mathbf{H}_{RE}^T\mathbf{W}_E\sqrt{\frac{\left(1-\phi\right)P_R}{N_R-2}}\mathbf{v}^{(2)} \end{aligned} \tag{64}$$

where $\mathbf{y}_E^{(\tau)} = \left[y_{E_1}^{(\tau)}\ y_{E_2}^{(\tau)} \cdots y_{E_{N_T}}^{(\tau)}\right]$ with $\tau = 1, 2$ representing the two phases, and $\mathbf{h}_{AE}$, $\mathbf{h}_{BE}$ and $\mathbf{H}_{RE}$ denote the channels from Users A and B and the relay to the multiple eavesdroppers, respectively. For notational simplicity, we denote $\mathbf{g}_A = \mathbf{H}_{RE}^T\mathbf{w}_A$, $\mathbf{g}_B = \mathbf{H}_{RE}^T\mathbf{w}_B$ and $\mathbf{G}_E = \mathbf{H}_{RE}^T\mathbf{W}_E$ in (64). Based on (64), the ergodic rate of s_{A2} at the eavesdroppers is given by

$$\begin{aligned} \bar{C}_{A2}^E &= \mathbb{E}_{\mathbf{g}_A, \mathbf{g}_B, \mathbf{G}_E}\left\{\frac{1}{2}\log_2\left|\mathbf{I} + \frac{\phi P_R}{2}\mathbf{g}_B\mathbf{g}_B^H\Big(\frac{\phi P_R}{2}\mathbf{g}_A\mathbf{g}_A^H \right.\right. \\ &\quad \left.\left. + \frac{\left(1-\phi\right)P_R}{N_R-2}\mathbf{G}_E\mathbf{G}_E^H\Big)^{-1}\right|\right\} \\ &= \frac{1}{2\ln 2}\mathbb{E}_{\mathbf{g}_A, \mathbf{g}_B, \mathbf{G}_E}\left\{\ln\left(1 + \frac{\phi}{2}\mathbf{g}_B^H\left(\frac{\phi}{2}\mathbf{g}_A\mathbf{g}_A^H \right.\right.\right. \\ &\quad \left.\left.\left. + \frac{(1-\phi)}{N_R-2}\mathbf{G}_E\mathbf{G}_E^H\right)^{-1}\mathbf{g}_B\right)\right\}. \end{aligned} \tag{65}$$

Following the similar transformation, the ergodic rates of the other symbols at the eavesdroppers can be expressed as

$$\bar{C}_{B2}^E = \frac{1}{2\ln 2}\mathbb{E}_{\mathbf{g}_A, \mathbf{G}_E}\left\{\ln\left(1 + \frac{\phi}{2}\mathbf{g}_A^H\Big(\frac{1-\phi}{N_R-2}\mathbf{G}_E^H\mathbf{G}_E\Big)^{-1}\mathbf{g}_A\right)\right\} \tag{66}$$

$$\begin{aligned} \bar{C}_{A1}^E = \frac{1}{2\ln 2}\mathbb{E}_{\mathbf{h}_{AE}, \mathbf{h}_{BE}, \mathbf{G}_E}\Big\{\ln\Big(1 + \alpha P_A\mathbf{h}_{AE}^H\Big(\alpha P_B\mathbf{h}_{BE}\mathbf{h}_{BE}^H \\ + \frac{P_R}{N_R-2}\mathbf{G}_E\mathbf{G}_E^H\Big)^{-1}\mathbf{h}_{AE}\Big)\Big\} \end{aligned} \tag{67}$$

$$\begin{aligned} \bar{C}_{B1}^E = \frac{1}{2\ln 2}\mathbb{E}_{\mathbf{h}_{BE}, \mathbf{G}_E}\Big\{\ln\Big(1 + \alpha P_B\mathbf{h}_{BE}^H \\ \Big(\frac{P_R}{N_R-2}\mathbf{G}_E\mathbf{G}_E^H\Big)^{-1}\mathbf{h}_{BE}\Big)\Big\}. \end{aligned} \tag{68}$$

For the channel related to the eavesdroppers, we assume that the entries in $\mathbf{h}_{AE}$, $\mathbf{h}_{BE}$ and $\mathbf{H}_{RE}$ are i.i.d zero-mean complex Gaussian variables with variances β_{AE}, β_{BE} and β_{RE}, respectively. Moreover, due to the unitarity of $\mathbf{W} = [\mathbf{w}_A\ \mathbf{w}_B\ \mathbf{W}_E]$, the entries of $\mathbf{H}_{RE}^T\mathbf{W} = [\mathbf{g}_A\ \mathbf{g}_B\ \mathbf{G}_E]$ are also the i.i.d. complex Gaussian variables with variance β_{RE}. Therefore, $\mathbf{h}_{AE}$, $\mathbf{h}_{BE}$, $\mathbf{g}_A$, $\mathbf{g}_B$ and $\mathbf{G}_E$ are independent of each other. As a result, $\eta_{A2}^E = \frac{\phi}{2}\mathbf{g}_B^H\left(\frac{\phi}{2}\mathbf{g}_A^H\mathbf{g}_A + \frac{(1-\phi)}{N_R-2}\mathbf{G}_E^H\mathbf{G}_E\right)^{-1}\mathbf{g}_B$ can be reagarded as the SINR of an N_E-branch MMSE linear diversity combiner operating in a Raleigh-fading channel with (N_R-1) interferers [57]. Then, the CCDF of η_{A2}^E is given by

$$\bar{F}_{\eta_{A2}^E} = \sum_{i=0}^{N_E-1}\Phi_i\frac{\left(\frac{2(1-\phi)}{\phi(N_R-2)}x\right)^i}{\left(1+\frac{2(1-\phi)}{\phi(N_R-2)}x\right)^{N_R-2}(x+1)} \tag{69}$$

where $\Phi_i = \binom{N_R-2}{i} + \binom{N_R-2}{i-1}$ for $i = 1,\ldots,N_E-1$ and $\Phi_0 = 1$. Similarly, by defining $\eta_{B2}^E = \frac{\phi}{2}\mathbf{g}_A^H\left(\frac{(1-\phi)}{N_R-2}\mathbf{G}_E^H\mathbf{G}_E\right)^{-1}\mathbf{g}_A$, $\eta_{A1}^E = \alpha P_A\mathbf{h}_{AE}^H\left(\alpha P_B\mathbf{h}_{BE}\mathbf{h}_{BE}^H + \frac{P_R}{N_R-2}\mathbf{G}_E\mathbf{G}_E^H\right)^{-1}\mathbf{h}_{AE}$, and $\eta_{B1}^E = \alpha P_B\mathbf{h}_{BE}^H\left(\frac{P_R}{N_R-2}\mathbf{G}_E\mathbf{G}_E^H\right)^{-1}\mathbf{h}_{BE}$, their CCDFs can be written as

$$\bar{F}_{\eta_{B2}^E} = \sum_{i=0}^{N_E-1}\binom{N_R-2}{i}\frac{\left(\frac{2(1-\phi)}{\phi(N_R-2)}x\right)^i}{\left(1+\frac{2(1-\phi)}{\phi(N_R-2)}x\right)^{N_R-2}} \tag{70}$$

$$\bar{F}_{\eta_{A1}^E} = \sum_{i=0}^{N_E-1}\Phi_i\frac{\left(\frac{P_R\beta_{RE}}{\alpha P_A\beta_{AE}(N_R-2)}x\right)^i}{\left(1+\frac{P_R\beta_{RE}}{\alpha P_A\beta_{AE}(N_R-2)}x\right)^{N_R-2}(x+1)} \tag{71}$$

$$\bar{F}_{\eta_{B1}^E} = \sum_{i=0}^{N_E-1}\binom{N_R-2}{i}\frac{\left(\frac{P_R\beta_{RE}}{\alpha P_B\beta_{BE}(N_R-2)}x\right)^i}{\left(1+\frac{P_R\beta_{RE}}{\alpha P_B\beta_{BE}(N_R-2)}x\right)^{N_R-2}}. \tag{72}$$

The ergodic rate of each data symbol in (65)–(68) at the colluding eavesdroppers can be further written as

$$\bar{C}_\delta^E = \frac{1}{2\ln 2}\int_0^\infty (1+x)\,f_{\eta_\delta^E}(x)dx = \frac{1}{2\ln 2}\int_0^\infty \frac{\bar{F}_{\eta_\delta^E}(x)}{1+x}dx \tag{73}$$

where $\delta \in \{A1, A2, B1, B2\}$. By substituting (69)–(72) into (73) and invoking [53, eq. (3.197.5)] to the integral parts, we can obtain

$$\bar{C}_{A1}^E = \frac{1}{2\ln 2}\Phi_i\left(\frac{P_R\beta_{RE}}{\alpha P_A\beta_{AE}(N_R-2)}\right)^i \mathrm{B}(i+1, N_R-i-1) \times {}_2F_1\left(N_R-2, i+1; N_R; 1-\frac{P_R\beta_{RE}}{\alpha P_A\beta_{AE}(N_R-2)}\right) \tag{74}$$

$$\bar{C}_{A2}^E = \frac{1}{2\ln 2}\Phi_i\left(\frac{2(1-\phi)}{\phi(N_R-2)}\right)^i \mathrm{B}(i+1, N_R-i-1) \times {}_2F_1\left(N_R-2, i+1; N_R; 1-\frac{2(1-\phi)}{\phi(N_R-2)}\right) \tag{75}$$

$$\bar{C}_{B1}^E = \frac{1}{2\ln 2}\sum_{i=0}^{N_E-1}\binom{N_R-2}{i} \times\left(\frac{P_R\beta_{RE}}{\alpha P_B\beta_{BE}(N_R-2)}\right)^i B(i+1, N_R-i) \times {}_2F_1\left(N_R-2, i+1; N_R-1; 1 - \frac{P_R\beta_{RE}}{\alpha P_B\beta_{BE}(N_R-2)}\right) \tag{76}$$

$$\bar{C}_{B2}^E = \frac{1}{2\ln 2}\sum_{i=0}^{N_E-1}\binom{N_R-2}{i} \times\left(\frac{2(1-\phi)}{\phi(N_R-2)}\right)^i B(i+1, N_R-i) \times {}_2F_1\left(N_R-2, i+1; N_R-1; 1-\frac{2(1-\phi)}{\phi(N_R-2)}\right). \tag{77}$$

With the results for the legitimate users in (38)–(41) and for the colluding eavesdroppers in (74)–(77), we can obtain the ergodic secrecy rate of each data symbol via (32) for the network under multiple colluding eavesdroppers.

V. Results and Analysis

In this section, we evaluate the performance of our proposed secure NOMA-based two-way relay network in terms of ergodic secrecy rate. In the simulations, we assume two legitimate users and the relay transmit with identical power, i.e., $P_A = P_B = P_R = P$ and the noise variance is identical at all nodes, i.e., $\sigma_A^2 = \sigma_B^2 = \sigma_R^2 = \sigma_E^2 = \sigma^2$. It is also assumed that the normalized gain of residual interference introduced by the full-duplex mode is identical at each legitimate user and the relay, i.e., $\beta_{AA} = \beta_{BB} = \beta_{RR} = \bar{\beta}$, where $0 \le \bar{\beta} \le 1$ [58]. The transmit SNR is defined as P/σ^2. As the links related to the relay are usually stronger than the links between users, we set $\beta_{AR} = \beta_{BR} = \beta_{RA} = \beta_{RB} = \beta_{RE} = 10$ and $\beta_{AB} = \beta_{BA} = \beta_{AE} = \beta_{BE} = 1$ in the simulations. In the following figures, we use A1, A2, B1, B2, A, B, and A + B to represent the ergodic secrecy rates of four data symbols s_{A1}, s_{A2}, s_{B1}, and s_{B2}, Users A and B, and the total network, respectively.

Fig. 2 shows the ergodic secrecy rates of different data symbols with respect to the normalized gain of self-interference $\bar{\beta}$, when $N_R = 3$, $N_E = 1$, $\alpha = 0.9$, $\phi = 0.5$, and SNR = 15 dB. Notably, Fig. 2 and the following figures demonstrate that the theoretical analysis of the ergodic secrecy rates in Sections III and IV is in perfect agreement with the simulation results. As seen from Fig. 2, the ergodic secrecy rate of each data symbol decreases as the normalized gain of self-interference $\bar{\beta}$ increases. This can be well understood since the strong self-interference has a negative effect on the decoding performance of the relay as well as the legitimate users during the first phase. However, even when the normalized gain of self-interference $\bar{\beta}$ is as high as 1, we can still obtain the positive results for all the ergodic secrecy rates, which implies that secure information exchange can always be guaranteed in our proposed network.

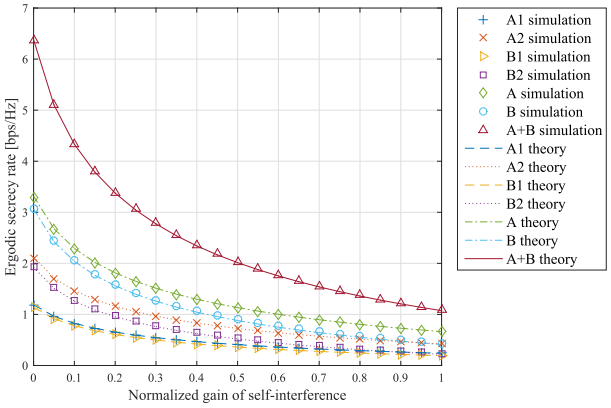

Fig. 2. Ergodic secrecy rate vs. normalized gain of self-interference $\bar{\beta}$ when $N_R = 3$, $N_E = 1$, $\alpha = 0.9$, $\phi = 0.5$, and SNR $= 15$ dB.

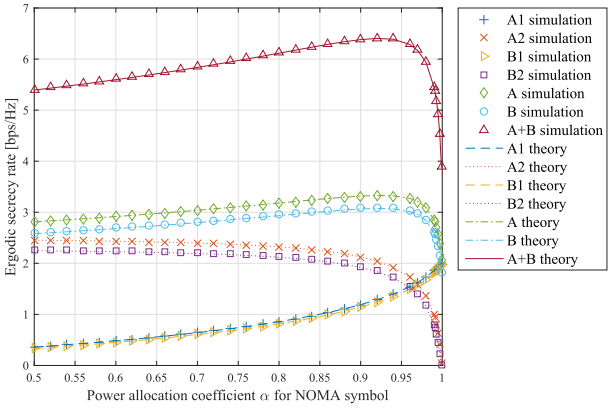

Fig. 3. Ergodic secrecy rate vs. power ratio α of NOMA symbols in (1) and (2) when $N_R = 3$, $N_E = 1$, $\phi = 0.5$, $\bar{\beta} = 0$, and SNR $= 15$ dB.

In Fig. 3, we show the ergodic secrecy rates of different data symbols with respect to the power ratio α of NOMA symbols in (1) and (2), where $N_R = 3$, $N_E = 1$, $\phi = 0.5$, $\bar{\beta} = 0$, and SNR $= 15$ dB. As seen from the figure, with the increase of the power ratio α of NOMA symbols, the ergodic secrecy rates of data symbols s_{A1} and s_{B1} increase while those of data symbols s_{A2} and s_{B2} decrease. On the other hand, Fig. 3 indicates that there exists an optimal value of α that maximizes the ergodic secrecy rates of Users A and B and the ergodic sum secrecy rate.

Fig. 4 shows the ergodic secrecy rates of different data symbols with respect to power allocation coefficient ϕ for the artificial noise scheme in (13), where $N_R = 3$, $N_E = 1$, $\alpha = 0.9$, $\bar{\beta} = 0.1$, and SNR $= 15$ dB. From the figure, we observe that an optimal value of ϕ exists to maximize the ergodic secrecy rates of data symbols s_{A2} and s_{B2} while the ergodic secrecy rates of data symbols s_{A1} and s_{B1} keep constant regardless of ϕ. Such phenomenon can be explained by the fact that the artificial noise scheme in (13) only contains data symbols s_{A2} and s_{B2}. Specially, when $\phi = 0$, the relay only broadcasts the pure jamming signals and data symbols s_{A2} and s_{B2} cannot be decoded in the second phase based on (25) and (26). When $\phi = 1$, the relay only forwards the data symbols s_{A2} and s_{B2} and no protection is afforded, which fails to guarantee the secure transmission of s_{B2}. As can be

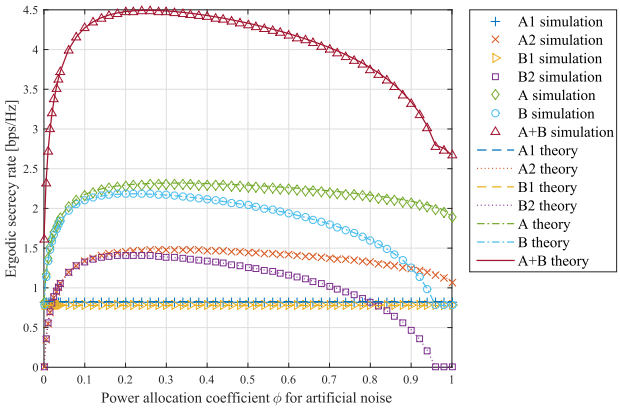

Fig. 4. Ergodic secrecy rate vs. power allocation coefficient ϕ for the artificial noise scheme in (13) when $N_R = 3$, $N_E = 1$, $\alpha = 0.9$, $\bar{\beta} = 0.1$, and SNR $= 15$ dB.

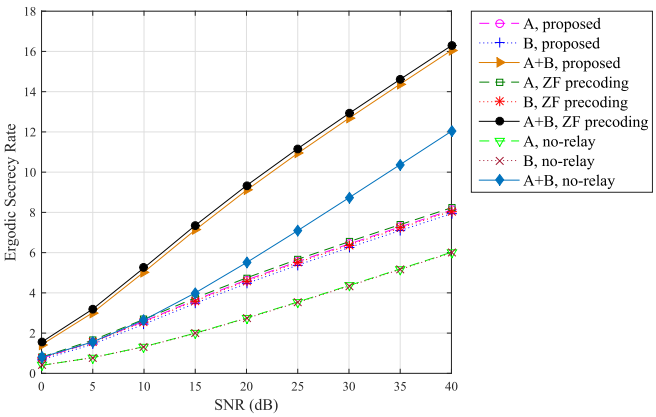

Fig. 5. Ergodic secrecy rates of different relay schemes vs. the transmit SNR when $N_R = 3$, $N_E = 1$, $\alpha = 0.9$, $\bar{\beta} = 0$, and $\phi = 0.3$.

seen, by choosing a proper ϕ, the network performance in terms of ergodic secrecy rate can be significantly improved.

In Fig. 5, we compare the ergodic secrecy rates of different relay schemes with respect to the transmit SNR, where $N_R = 3$, $N_E = 1$, $\alpha = 0.9$, $\bar{\beta} = 0$, and $\phi = 0.3$. As can be seen, by using the ZF precoding to replace the range space $\mathbf{W}_U$ at the relay, the network only achieves a secrecy performance that is marginally better than that of using the range space $\mathbf{W}_U$ in (3). Therefore, for simplicity, we mainly focus on the performance analysis of our proposed scheme. On the other hand, the proposed two-way network achieves a significant performance gain over the network without a relay, which corroborates the important role of the relay for security enhancements.

In Fig. 6, we compare the network performance under multiple eavesdroppers with the non-colluding and colluding manners with respect to the transmit SNR, where $N_R = 5$, $N_E = 2$, $\alpha = 0.9$, $\phi = 0.5$, and $\bar{\beta} = 0.1$. As can be observed, the network performance under the colluding eavesdroppers is worse than that under the non-colluding eavesdroppers. It can be well understood since by jointly processing the received signals at multiple eavesdroppers, colluding manner can wiretap more information than the non-colluding one, leading to worse secure performance for the proposed network.

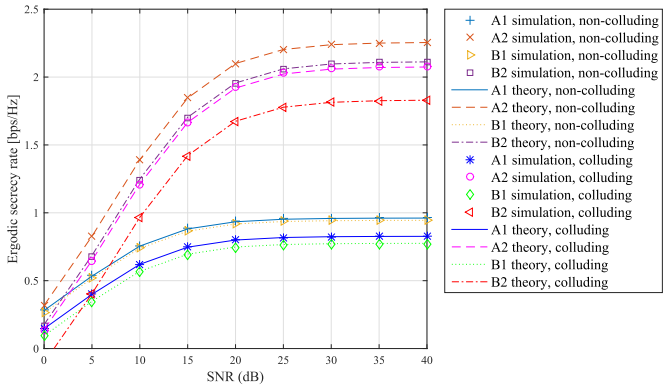

Fig. 6. Ergodic secrecy rates under non-colluding and colluding manners vs. the transmit SNR when $N_R = 5$, $N_E = 2$, $\alpha = 0.9$, $\phi = 0.5$, and $\bar{\beta} = 0.1$.

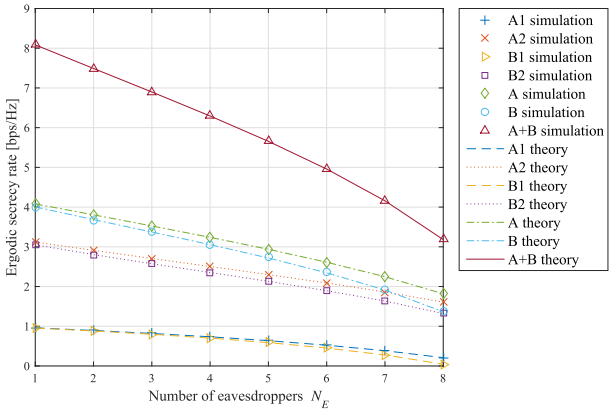

Fig. 7. Ergodic secrecy rate vs. number of eavesdroppers N_E when $N_R = 12$, $\alpha = 0.9$, $\phi = 0.5$, $\bar{\beta} = 0.1$, and SNR $= 30$ dB.

Fig. 7 shows the ergodic secrecy rates of different data symbols with respect to the number of eavesdroppers N_E, where $N_R = 12$, $\alpha = 0.9$, $\phi = 0.5$, $\bar{\beta} = 0.1$, and SNR $= 30$ dB. Considering multiple eavesdroppers with colluding manner, we observe that the ergodic secrecy rates of different data symbols decrease as the number of eavesdroppers N_E increases. This adverse effect is caused by the improvement of the eavesdropping ability with the increasing number of eavesdroppers.

In Fig. 8, we show the ergodic secrecy rates of different data symbols with respect to the number of antennas N_R at the relay, where $N_E = 2$, $\alpha = 0.9$, $\phi = 0.5$, $\bar{\beta} = 0.1$, and SNR $= 30$ dB. As can be seen, the ergodic secrecy rates of different data symbols increase as the number of antennas N_R increases at the relay. However, the performance improvement of data symbols s_{A1} and s_{B1} is marginal when increasing the number of antennas N_R at the relay beyond $N_R = 5$. It should be noted that the decoding of both data symbols s_{A1} and s_{B1} in (19)–(20) and (23)–(24) is associated with the user-to-relay link and the user-to-user link, respectively. Since the user-to-user link is much weaker and the decoding performance of data symbols s_{A1} and s_{B1} is almost limited by it, increasing the number of antennas N_R at the relay does not improve the user-to-user link as well as their decoding performance. On the other hand, we observe significant performance improvement of data symbols s_{A2} and s_{B2} as the number of antennas N_R increases at the relay, which is attributed to the reliable enhancement of the links between the relay and the users.

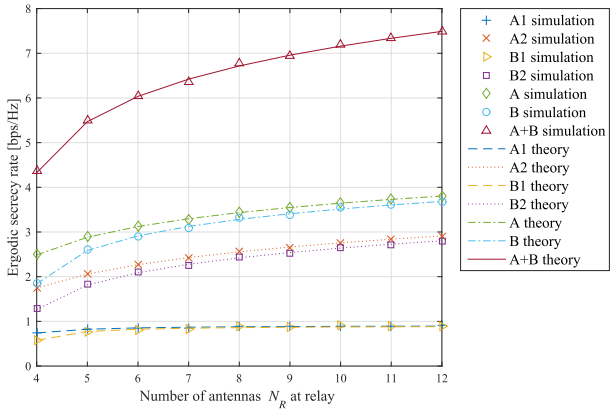

Fig. 8. Ergodic secrecy rate vs. number of antennas N_R at the relay when $N_E = 2$, $\alpha = 0.9$, $\phi = 0.5$, $\bar{\beta} = 0.1$, and SNR $= 30$ dB.

VI. Conclusions

In this paper, a novel secure NOMA-based two-way relay network has been proposed with the considerations of different eavesdropping cases. Specifically, by employing the full-duplex and the artificial noise techniques at the relay, we have enhanced the ability of the relay to combat the eavesdropping without impairing the legitimate users for ensuring secure information exchange. On the other hand, with the full-duplex mode applied to the user nodes in the first phase, we have improved the data transmission efficiency without requiring any extra bandwidth resource. Moreover, we have designed different decoding strategies based on SIC for different types of nodes, in which we have provided the eavesdroppers with a sophisticated strategy with jointly processing to examine the secure performance of the proposed network in the harsh wiretap condition. Finally, we have analyzed the performance of the secure NOMA-based two-way relay network and derived the closed-form expressions for the ergodic secrecy rates under single eavesdropper, multiple non-colluding, and colluding eavesdroppers. The theoretical derivations have been shown to agree with the simulation results perfectly. Our future concerns will be the enhancement design of secure NOMA-based networks and the optimization problems on the power allocations for the NOMA symbols and the artificial noise scheme in the proposed network.

Appendix A
Proof of Proposition 1

Letting $\eta_{A1} = \min\left\{\frac{\beta_{AR}\rho_A}{P_R\beta_{RR}+\sigma_R^2}, \frac{|h_{AB}|^2}{P_B\beta_{BB}+\sigma_B^2}\right\}$ in (33), and using the CCDF of ρ_A in (9) and the CCDF of $|h_{AB}|^2$ as $\bar{F}_{|h_{AB}|^2}(x) = \exp\left(-\frac{x}{\beta_{AB}}\right)$, we can obtain the CCDF of η_{A1} as

$$\begin{aligned}\bar{F}_{\eta_{A1}}(x) &= \Pr\left\{\frac{\beta_{AR}\rho_A}{P_R\beta_{RR}+\sigma_R^2} > x, \frac{|h_{AB}|^2}{P_B\beta_{BB}+\sigma_B^2} > x\right\} \\ &= \bar{F}_{\rho_A}\left(\frac{P_R\beta_{RR}+\sigma_R^2}{\beta_{AR}}x\right)\bar{F}_{|h_{AB}|^2}\left(\left(P_B\beta_{BB}+\sigma_B^2\right)x\right) \\ &= \exp\left(-\left(\frac{P_R\beta_{RR}+\sigma_R^2}{\beta_{AR}}+\frac{P_B\beta_{BB}+\sigma_B^2}{\beta_{AB}}\right)x\right) \\ &\quad\times\sum_{k=0}^{N_R-2}\frac{\left(\frac{P_R\beta_{RR}+\sigma_R^2}{\beta_{AR}}x\right)^k}{k!}. \end{aligned} \tag{78}$$

With (78), the ergodic rate of s_{A1} can be derived as

$$\begin{aligned}\bar{C}_{A1} &= \int_0^\infty \frac{1}{2}\left(\log_2\left(1+P_A x\right)\right.\\ &\quad \left.-\log_2\left(1+(1-\alpha)P_A x\right)\right) f_{\eta_{A1}}(x)dx\\ &= \frac{1}{2\ln 2}\left(\int_0^\infty \ln\left(1+P_A x\right) f_{\eta_{A1}}(x)dx\right.\\ &\quad \left.-\int_0^\infty \ln\left(1+(1-\alpha)P_A x\right) f_{\eta_{A1}}(x)dx\right)\\ &= \frac{1}{2\ln 2}\left(P_A\int_0^\infty \frac{\bar{F}_{\eta_{A1}}(x)}{1+P_A x}dx\right.\\ &\quad \left.-(1-\alpha)P_A\int_0^\infty \frac{\bar{F}_{\eta_{A1}}(x)}{1+(1-\alpha)P_A x}dx\right)\\ &= \frac{1}{2\ln 2}\sum_{k=0}^{N_R-2}\frac{\left(\frac{P_R\beta_{RR}+\sigma_R^2}{\beta_{AR}}\right)^k}{k!}\\ &\quad \times\left(\int_0^\infty \frac{\exp\left(-\left(\frac{P_R\beta_{RR}+\sigma_R^2}{\beta_{AR}}+\frac{P_B\beta_{BB}+\sigma_B^2}{\beta_{AB}}\right)x\right)}{\frac{1}{P_A}+x}x^k dx\right.\\ &\quad \left.-\int_0^\infty \frac{\exp\left(-\left(\frac{P_R\beta_{RR}+\sigma_R^2}{\beta_{AR}}+\frac{P_B\beta_{BB}+\sigma_B^2}{\beta_{AB}}\right)x\right)x^k}{\frac{1}{(1-\alpha)P_A}+x}dx\right).\end{aligned} \tag{79}$$

By applying [53, eq. (3.353.5)] to the integral parts in (79), we finally obtain (38).

APPENDIX B
PROOF OF PROPOSITION 2

Let $\eta_{A2} = \min\left\{\frac{(1-\alpha)P_A\beta_{AR}\rho_A}{P_R\beta_{RR}+\sigma_R^2}, \frac{\left|\mathbf{h}_{RB}^T\mathbf{w}_B\right|^2\phi P_R}{2\sigma_B^2}\right\}$ in (35).

As $\mathbf{w}_B$ is one column of the orthonormal basis $\mathbf{W}$, it can be readily verified that $\mathbf{h}_{RB}^T\mathbf{w}_B$ follows the zero-mean complex Gaussian distribution with variance β_{RB} and we have the CCDF of $\left|\mathbf{h}_{RB}^T\mathbf{w}_B\right|^2$ as $\bar{F}_{\left|\mathbf{h}_{RB}^T\mathbf{w}_B\right|^2}(x) = \exp\left(-\frac{x}{\beta_{RB}}\right)$. With the CCDF of ρ_A given in (9), we can obtain the CCDF of η_{A2} as

$$\begin{aligned}\bar{F}_{\eta_{A2}}(x) &= \Pr\left\{\frac{(1-\alpha)P_A\beta_{AR}\rho_A}{P_R\beta_{RR}+\sigma_R^2}>x, \frac{\left|\mathbf{h}_{RB}^T\mathbf{w}_B\right|^2\phi P_R}{2\sigma_B^2}>x\right\}\\ &= \bar{F}_{\rho_A}\left(\frac{P_R\beta_{RR}+\sigma_R^2}{(1-\alpha)P_A\beta_{AR}}x\right)\bar{F}_{\left|\mathbf{h}_{RB}^T\mathbf{w}_B\right|^2}\left(\frac{2\sigma_B^2}{\phi P_R}x\right)\\ &= \exp\left(-\left(\frac{P_R\beta_{RR}+\sigma_R^2}{(1-\alpha)P_A\beta_{AR}}+\frac{2\sigma_B^2}{\phi P_R\beta_{RB}}\right)x\right)\\ &\quad\times\sum_{k=0}^{N_R-2}\frac{\left(\frac{P_R\beta_{RR}+\sigma_R^2}{(1-\alpha)P_A\beta_{AR}}x\right)^k}{k!}.\end{aligned} \tag{80}$$

With (80), the ergodic rate of s_{A2} can be written as

$$\begin{aligned}\bar{C}_{A2} &= \int_0^\infty \frac{1}{2}\log_2\left(1+x\right) f_{\eta_{A2}}(x)dx\\ &= \frac{1}{2\ln 2}\int_0^\infty \frac{\bar{F}_{\eta_{A2}}(x)}{1+x}dx.\end{aligned} \tag{81}$$

As (80) has a similar form to (78), after substituting (80) into (81) and applying [53, eq. (3.353.5)] to the integral part, we can finally obtain (40).

APPENDIX C
PROOF OF PROPOSITION 3

Let us denote $\mathbf{g}^T = \left[g_A\ g_B\ \mathbf{g}_E^T\right]^T = \mathbf{h}_{RE}^T\mathbf{W}$. We can obtain $\mathbf{g} \sim \mathcal{N}_c(\mathbf{0}_{N_R\times 1}, \beta_{RE}\mathbf{I}_{N_R})$, which has i.i.d. complex Gaussian entries as $\mathbf{W}$ is a unitary matrix. By denoting $v_A = \frac{|g_A|^2}{\beta_{RE}} = \frac{\left|\mathbf{h}_{RE}^T\mathbf{w}_A\right|^2}{\beta_{RE}}$, $v_B = \frac{|g_B|^2}{\beta_{RE}} = \frac{\left|\mathbf{h}_{RE}^T\mathbf{w}_B\right|^2}{\beta_{RE}}$, and $v_E = \frac{\|\mathbf{g}_E\|^2}{\beta_{RE}} = \frac{\left\|\mathbf{h}_{RE}^T\mathbf{W}_E\right\|^2}{\beta_{RE}}$, we have $v_A \sim \exp(1)$, $v_B \sim \exp(1)$, and $v_E \sim \Gamma\left(N_R-2,1\right)$, where $\Gamma\left(\alpha,x\right)$ is the upper incomplete gamma function [53, eq. (8.350.2)]. Then, we can derive the CCDF of γ_{A2}^E in (27) as

$$\begin{aligned}\bar{F}_{\gamma_{A2}^E} &= \Pr\left\{\frac{\phi\left(N_R-2\right)v_A}{\phi\left(N_R-2\right)v_B+2\left(1-\phi\right)v_E+\frac{2(N_R-2)\sigma_E^2}{P_R\beta_{RE}}}>x\right\}\\ &= \Pr\left\{v_A > \left(v_B+\frac{2\left(1-\phi\right)v_E}{\phi\left(N_R-2\right)}+\frac{2\sigma_E^2}{\phi P_R\beta_{RE}}\right)x\right\}\\ &= \mathbb{E}_{v_E,v_B}\left[\exp\left(-\left(v_B+\frac{2\left(1-\phi\right)v_E}{\phi\left(N_R-2\right)}+\frac{2\sigma_E^2}{\phi P_R\beta_{RE}}\right)x\right)\right]\\ &= \int_0^\infty\int_0^\infty \exp\left(-\left(v_B+\frac{2\left(1-\phi\right)v_E}{\phi\left(N_R-2\right)}+\frac{2\sigma_E^2}{\phi P_R\beta_{RE}}\right)x\right)\\ &\quad\times\left(v_E\right)^{N_R-3}\frac{\exp\left(-v_E\right)}{\left(N_R-3\right)!}\exp\left(-v_B\right)dv_E dv_B\\ &= \frac{\exp\left(-\frac{2\sigma_E^2}{\phi P_R\beta_{RE}}x\right)}{\left(1+\frac{2(1-\phi)}{\phi(N_R-2)}x\right)^{2-N_R}\left(x+1\right)^{-1}}\end{aligned} \tag{82}$$

where the double integral is solved by using the formulas [53, eq. (3.381.3)] and [53, eq. (3.310)]. With (82), the ergodic rate of s_{A2} at the eavesdropper can be derived as

$$\begin{aligned}\bar{C}_{A2}^E &= \frac{1}{2\ln 2}\int_0^\infty \frac{\bar{F}_{\gamma_{A2}^E}(x)}{1+x}dx\\ &= \frac{1}{2\ln 2}\int_0^\infty \frac{\exp\left(-\frac{2\sigma_E^2}{\phi P_R\beta_{RE}}x\right)}{\left(1+\frac{2(1-\phi)}{\phi(N_R-2)}x\right)^{N_R-2}\left(x+1\right)^2}dx\\ &= \frac{1}{2\ln 2}\left(\sum_{i=1}^{N_R-2}\int_0^\infty \frac{\Omega_{A2}^i\exp\left(-\frac{2\sigma_E^2}{\phi P_R\beta_{RE}}x\right)}{\left(x+\frac{\phi(N_R-2)}{2(1-\phi)}\right)^i}dx\right.\\ &\quad\left.+\sum_{i=1}^{2}\int_0^\infty \frac{\Psi_{A2}^i\exp\left(-\frac{2\sigma_E^2}{\phi P_R\beta_{RE}}x\right)}{\left(x+1\right)^i}dx\right)\end{aligned} \tag{83}$$

where (83) is obtained by using the partial-fraction expansion [54, appendix], and Ω_{A2}^i and Ψ_{A2}^i are given in (45) and (46), respectively. By applying [53, eq. (3.353.2)] to the integral parts in (83), we finally obtain (44).

REFERENCES

[1] L. Dai, B. Wang, Y. Yuan, S. Han, C.-L. I, and Z. Wang, "Non-orthogonal multiple access for 5G: Solutions, challenges, opportunities, and future research trends," *IEEE Commun. Mag.*, vol. 53, no. 9, pp. 74–81, Sep. 2015.

[2] F. Zhou, Y. Wu, R. Q. Hu, Y. Wang, and K. K. Wong, "Energy-efficient NOMA enabled heterogeneous cloud radio access networks," *IEEE Netw.*, vol. 32, no. 2, pp. 152–160, Mar./Apr. 2018.

[3] Z. Ding *et al.*, "Application of non-orthogonal multiple access in LTE and 5G networks," *IEEE Commun. Mag.*, vol. 55, no. 2, pp. 185–191, Feb. 2017.

[4] Y. Saito, Y. Kishiyama, A. Benjebbour, T. Nakamura, A. Li, and K. Higuchi, "Non-orthogonal multiple access (NOMA) for cellular future radio access," in *Proc. IEEE VTC Spring*, Dresden, Germany, Jun. 2013, pp. 1–5.

[5] Y. Saito, A. Benjebbour, Y. Kishiyama, and T. Nakamura, "System-level performance evaluation of downlink non-orthogonal multiple access (NOMA)," in *Proc. IEEE PIMRC*, London, U.K., Sep. 2013, pp. 611–615.

[6] M. Al-Imari, P. Xiao, M. A. Imran, and R. Tafazolli, "Uplink non-orthogonal multiple access for 5G wireless networks," in *Proc. 11th Int. Symp. Wireless Commun. Sys.*, Aug. 2014, pp. 781–785.

[7] Z. Ding, Z. Yang, P. Fan, and H. V. Poor, "On the performance of non-orthogonal multiple access in 5G systems with randomly deployed users," *IEEE Signal Process. Lett.*, vol. 21, no. 12, pp. 1501–1505, Dec. 2014.

[8] S. Timotheou and I. Krikidis, "Fairness for non-orthogonal multiple access in 5G systems," *IEEE Signal Process. Lett.*, vol. 22, no. 10, pp. 1647–1651, Oct. 2015.

[9] J. Choi, "Minimum power multicast beamforming with superposition coding for multiresolution broadcast and application to NOMA systems," *IEEE Trans. Commun.*, vol. 63, no. 3, pp. 791–800, Mar. 2015.

[10] M. F. Hanif, Z. Ding, T. Ratnarajah, and G. K. Karagiannidis, "A minorization-maximization method for optimizing sum rate in the downlink of non-orthogonal multiple access systems," *IEEE Trans. Signal Process.*, vol. 64, no. 1, pp. 76–88, Jan. 2016.

[11] Z. Ding, F. Adachi, and H. V. Poor, "The application of MIMO to non-orthogonal multiple access," *IEEE Trans. Wireless Commun.*, vol. 15, no. 1, pp. 537–552, Jan. 2016.

[12] Z. Ding *et al.*, "Impact of user pairing on 5G nonorthogonal multiple-access downlink transmissions," *IEEE Trans. Veh. Technol.*, vol. 65, no. 8, pp. 6010–6023, Aug. 2016.

[13] Y. Liu, Z. Ding, M. Elkashlan, and J. Yuan, "Nonorthogonal multiple access in large-scale underlay cognitive radio networks," *IEEE Trans. Veh. Technol.*, vol. 65, no. 12, pp. 10152–10157, Dec. 2016.

[14] L. Lv, J. Chen, Q. Ni, and Z. Ding, "Design of cooperative non-orthogonal multicast cognitive multiple access for 5G systems: User scheduling and performance analysis," *IEEE Trans. Commun.*, vol. 65, no. 6, pp. 2641–2656, Jun. 2017.

[15] X. Liang, Y. Wu, D. W. K. Ng, Y. Zuo, S. Jin, and H. Zhu, "Outage performance for cooperative NOMA transmission with an AF relay," *IEEE Commun. Lett.*, vol. 21, no. 11, pp. 2428–2431, Nov. 2017.

[16] Z. Ding, M. Peng, and H. V. Poor, "Cooperative non-orthogonal multiple access in 5G systems," *IEEE Commun. Lett.*, vol. 19, no. 8, pp. 1462–1465, Aug. 2015.

[17] J.-B. Kim and I.-H. Lee, "Capacity analysis of cooperative relaying systems using non-orthogonal multiple access," *IEEE Commun. Lett.*, vol. 19, no. 11, pp. 1949–1952, Nov. 2015.

[18] B. Zheng, X. Wang, M. Wen, and F. Chen, "NOMA-based multi-pair two-way relay networks with rate splitting and group decoding," *IEEE J. Sel. Areas Commun.*, vol. 35, no. 10, pp. 2328–2341, Oct. 2017.

[19] A. D. Wyner, "The wire-tap channel," *Bell Syst. Tech. J.*, vol. 54, no. 8, pp. 1355–1387, 1975.

[20] Y. Wu, J.-B. Wang, J. Wang, R. Schober, and C. Xiao, "Secure transmission with large numbers of antennas and finite alphabet inputs," *IEEE Trans. Commun.*, vol. 65, no. 8, pp. 3614–3628, Aug. 2017.

[21] Y. Wu, R. Schober, D. W. K. Ng, C. Xiao, and G. Caire, "Secure massive MIMO transmission with an active eavesdropper," *IEEE Trans. Inf. Theory*, vol. 62, no. 7, pp. 3880–3900, Jul. 2016.

[22] A. Khina, Y. Kochman, and A. Khisti, "The MIMO wiretap channel decomposed," *IEEE Trans. Inf. Theory*, vol. 64, no. 2, pp. 1046–1063, Feb. 2018.

[23] S. Shafiee and S. Ulukus, "Achievable rates in Gaussian MISO channels with secrecy constraints," in *Proc. IEEE ISIT*, Nice, France, Jun. 2007, pp. 2466–2470.

[24] A. Khisti and G. W. Wornell, "Secure transmission with multiple antennas I: The MISOME wiretap channel," *IEEE Trans. Inf. Theory*, vol. 56, no. 7, pp. 3088–3104, Jul. 2010.

[25] A. Khisti and G. W. Wornell, "Secure transmission with multiple antennas—Part II: The MIMOME wiretap channel," *IEEE Trans. Inf. Theory*, vol. 56, no. 11, pp. 5515–5532, Nov. 2010.

[26] T. Liu and S. Shamai (Shitz), "A note on the secrecy capacity of the multiple-antenna wiretap channel," *IEEE Trans. Inf. Theory*, vol. 55, no. 6, pp. 2547–2553, Jun. 2009.

[27] F. Oggier and B. Hassibi, "The secrecy capacity of the MIMO wiretap channel," *IEEE Trans. Inf. Theory*, vol. 57, no. 8, pp. 4961–4972, Aug. 2011.

[28] S. Goel and R. Negi, "Guaranteeing secrecy using artificial noise," *IEEE Trans. Wireless Commun.*, vol. 7, no. 6, pp. 2180–2189, Jun. 2008.

[29] T.-X. Zheng, H.-M. Wang, J. Yuan, D. Towsley, and M. H. Lee, "Multi-antenna transmission with artificial noise against randomly distributed eavesdroppers," *IEEE Trans. Commun.*, vol. 63, no. 11, pp. 4347–4362, Nov. 2015.

[30] H.-M. Wang, T. Zheng, and X.-G. Xia, "Secure MISO wiretap channels with multiantenna passive eavesdropper: Artificial noise vs. artificial fast fading," *IEEE Trans. Wireless Commun.*, vol. 14, no. 1, pp. 94–106, Jan. 2015.

[31] X. Zhou and M. R. McKay, "Secure transmission with artificial noise over fading channels: Achievable rate and optimal power allocation," *IEEE Trans. Veh. Technol.*, vol. 59, no. 8, pp. 3831–3842, Oct. 2010.

[32] X. Zhang, X. Zhou, and M. R. McKay, "On the design of artificial-noise-aided secure multi-antenna transmission in slow fading channels," *IEEE Trans. Veh. Technol.*, vol. 62, no. 5, pp. 2170–2181, Jun. 2013.

[33] C. Wang, H.-M. Wang, and X.-G. Xia, "Hybrid opportunistic relaying and jamming with power allocation for secure cooperative networks," *IEEE Trans. Wireless Commun.*, vol. 14, no. 2, pp. 589–605, Feb. 2015.

[34] C. Wang, H.-M. Wang, D. W. K. Ng, X.-G. Xia, and C. Liu, "Joint beamforming and power allocation for secrecy in peer-to-peer relay networks," *IEEE Trans. Wireless Commun.*, vol. 14, no. 6, pp. 3280–3293, Jun. 2015.

[35] M. Yang, B. Zhang, Y. Huang, N. Yang, D. B. da Costa, and D. Guo, "Secrecy enhancement of multiuser MISO networks using OSTBC and artificial noise," *IEEE Trans. Veh. Technol.*, vol. 66, no. 12, pp. 11394–11398, Dec. 2017.

[36] H.-M. Wang, M. Luo, Q. Yin, and X.-G. Xia, "Hybrid cooperative beamforming and jamming for physical-layer security of two-way relay networks," *IEEE Trans. Inf. Forensics Security*, vol. 8, no. 12, pp. 2007–2020, Dec. 2013.

[37] J. Chen, R. Zhang, L. Song, Z. Han, and B. Jiao, "Joint relay and jammer selection for secure two-way relay networks," *IEEE Trans. Inf. Forensics Security*, vol. 7, no. 1, pp. 310–320, Feb. 2012.

[38] X. Ding, T. Song, Y. Zou, X. Chen, and L. Hanzo, "Security-reliability tradeoff analysis of artificial noise aided two-way opportunistic relay selection," *IEEE Trans. Veh. Technol.*, vol. 66, no. 5, pp. 3930–3941, May 2017.

[39] Y. Liu, Z. Qin, M. Elkashlan, Y. Gao, and L. Hanzo, "Enhancing the physical layer security of non-orthogonal multiple access in large-scale networks," *IEEE Trans. Wireless Commun.*, vol. 16, no. 3, pp. 1656–1672, Mar. 2017.

[40] Z. Qin, Y. Liu, Z. Ding, Y. Gao, and M. Elkashlan, "Physical layer security for 5G non-orthogonal multiple access in large-scale networks," in *Proc. IEEE Int. Conf. Commun.*, Kuala Lumpur, Malaysia, May 2016, pp. 1–6.

[41] Z. Ding, Z. Zhao, M. Peng, and H. V. Poor, "On the spectral efficiency and security enhancements of NOMA assisted multicast-unicast streaming," *IEEE Trans. Commun.*, vol. 65, no. 7, pp. 3151–3163, Jul. 2017.

[42] B. He, A. Liu, N. Yang, and V. K. N. Lau, "On the design of secure non-orthogonal multiple access systems," *IEEE J. Sel. Areas Commun.*, vol. 35, no. 10, pp. 2196–2206, Oct. 2017.

[43] Y. Zhang, H.-M. Wang, Q. Yang, and Z. Ding, "Secrecy sum rate maximization in non-orthogonal multiple access," *IEEE Commun. Lett.*, vol. 20, no. 5, pp. 930–933, May 2016.

[44] Y. Li, M. Jiang, Q. Zhang, Q. Li, and J. Qin, "Secure beamforming in downlink MISO non-orthogonal multiple access systems," *IEEE Trans. Veh. Technol.*, vol. 66, no. 8, pp. 7563–7567, Aug. 2017.

[45] M. Tian, Q. Zhang, S. Zhao, Q. Li, and J. Qin, "Secrecy sum rate optimization for downlink MIMO nonorthogonal multiple access systems," *IEEE Signal Process. Lett.*, vol. 24, no. 8, pp. 1113–1117, Aug. 2017.

[46] J. Tang, D. K. C. So, A. Shojaeifard, K.-K. Wong, and J. Wen, "Joint antenna selection and spatial switching for energy efficient MIMO SWIPT system," *IEEE Trans. Wireless Commun.*, vol. 16, no. 7, pp. 4754–4769, Jul. 2017.

[47] Y. Jiang, M. K. Varanasi, and J. Li, "Performance analysis of ZF and MMSE equalizers for MIMO systems: An in-depth study of the high SNR regime," *IEEE Trans. Inf. Theory*, vol. 57, no. 4, pp. 2008–2026, Apr. 2011.

[48] T. W. Anderson, T. W. Anderson, T. W. Anderson, T. W. Anderson, and E.-U. Mathématicien, *An Introduction to Multivariate Statistical Analysis*, vol. 2. New York, NY, USA: Wiley, 1958.
[49] D. Korpi *et al.*, "Full-duplex mobile device: Pushing the limits," *IEEE Commun. Mag.*, vol. 54, no. 9, pp. 80–87, Sep. 2016.
[50] L. Wang, F. Tian, T. Svensson, D. Feng, M. Song, and S. Li, "Exploiting full duplex for device-to-device communications in heterogeneous networks," *IEEE Commun. Mag.*, vol. 53, no. 5, pp. 146–152, May 2015.
[51] A. Sabharwal, P. Schniter, D. Guo, D. W. Bliss, S. Rangarajan, and R. Wichman, "In-band full-duplex wireless: Challenges and opportunities," *IEEE J. Sel. Areas Commun.*, vol. 32, no. 9, pp. 1637–1652, Sep. 2014.
[52] P. K. Gopala, L. Lai, and H. El Gamal, "On the secrecy capacity of fading channels," *IEEE Trans. Inf. Theory*, vol. 54, no. 10, pp. 4687–4698, Oct. 2008.
[53] I. S. Gradshteyn and I. M. Ryzhik, *Table of Integrals, Series, and Products*, 7th ed. San Diego, CA, USA: Academic, 2007.
[54] A. V. Oppenheim, A. Willsky, and S. Nawab, *Signals and Systems*, 2nd ed. Englewood Cliffs, NJ, USA: Prentice-Hall, 1997.
[55] W. Wang, K. C. Teh, and K. H. Li, "Secrecy throughput maximization for MISO multi-eavesdropper wiretap channels," *IEEE Trans. Inf. Forensics Security*, vol. 12, no. 3, pp. 505–515, Mar. 2017.
[56] T.-X. Zheng, H.-M. Wang, and Q. Yin, "On transmission secrecy outage of a multi-antenna system with randomly located eavesdroppers," *IEEE Commun. Lett.*, vol. 18, no. 8, pp. 1299–1302, Aug. 2014.
[57] H. Gao, P. J. Smith, and M. V. Clark, "Theoretical reliability of MMSE linear diversity combining in Rayleigh-fading additive interference channels," *IEEE Trans. Commun.*, vol. 46, no. 5, pp. 666–672, May 1998.
[58] A. Mukherjee and A. L. Swindlehurst, "A full-duplex active eavesdropper in MIMO wiretap channels: Construction and countermeasures," in *Proc. Conf. Signals, Syst. Comput. (ASILOMAR)*, Pacific Grove, CA, USA, Nov. 2011, pp. 265–269.

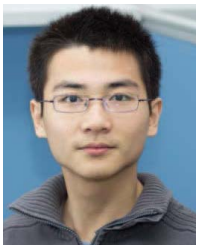

Beixiong Zheng received the B.S. degree from the South China University of Technology, Guangzhou, China, in 2013. He is currently pursuing the Ph.D. degree with the South China University of Technology, Guangzhou. His recent research interests include index modulation, non-orthogonal multiple access, and pilot multiplexing techniques.

From 2015 to 2016, he was a Visiting Student Research Collaborator with Columbia University, New York, NY, USA. He received the Best Paper Award from the IEEE International Conference on Computing, Networking and Communications in 2016.

Miaowen Wen (M'14–SM'18) received the B.S. degree from Beijing Jiaotong University, Beijing, China, in 2009, and the Ph.D. degree from Peking University, Beijing, China, in 2014. From 2012 to 2013, he was a Visiting Student Research Collaborator with Princeton University, Princeton, NJ, USA. He is currently an Associate Professor with the South China University of Technology, Guangzhou, China. He has authored a book and over 80 papers in refereed journals and conference proceedings. His research interests include index modulation, non-orthogonal multiple access, physical layer security, and molecular communications.

Dr. Wen was a recipient of the Excellent Doctoral Dissertation Award from Peking University and the Best Paper Awards from the IEEE ITST 2012, the IEEE ITSC 2014, and the IEEE ICNC 2016. He was recognized as an Exemplary Reviewer for the IEEE COMMUNICATIONS LETTERS in 2017. He currently serves as a Symposium Co-Chair for the IEEE ICNC'2019, a Workshop Co-Chair for the IEEE ICCC'2018, and on the Editorial Boards of several international journals, including IEEE ACCESS, *EURASIP Journal on Wireless Communications and Networking*, *ETRI Journal*, and *Physical Communication* (Elsevier).

Cheng-Xiang Wang (S'01–M'05–SM'08–F'17) received the B.Sc. and M.Eng. degrees in communication and information systems from Shandong University, China, in 1997 and 2000, respectively, and the Ph.D. degree in wireless communications from Aalborg University, Denmark, in 2004.

He has been with Heriot-Watt University, Edinburgh, U.K., since 2005, and became a Professor of wireless communications in 2011. He is also an Honorary Fellow with the University of Edinburgh, U.K., a Chair Professor with Shandong University, and a Guest Professor with Southeast University, China. He was a Research Fellow with the University of Agder, Grimstad, Norway, from 2001 to 2005, a Visiting Researcher with Siemens AG-Mobile Phones, Munich, Germany, in 2004, and a Research Assistant with the Hamburg University of Technology, Hamburg, Germany, from 2000 to 2001. He has co-authored two books, one book chapter, and over 320 papers in refereed journals and conference proceedings. His current research interests include wireless channel measurements/modeling and (B)5G wireless communication networks, including green communications, cognitive radio networks, high mobility communication networks, massive MIMO, millimeter wave communications, and visible light communications.

Prof. Wang is a fellow of the IET and HEA. He has served as a Technical Program Committee (TPC) Member, TPC Chair, and the General Chair for over 80 international conferences. He is recognized as a Web of Science 2017 Highly Cited Researcher. He received nine Best Paper Awards from the IEEE Globecom 2010, the IEEE ICCT 2011, ITST 2012, the IEEE VTC 2013-Spring, IWCMC 2015, IWCMC 2016, the IEEE/CIC ICCC 2016, and WPMC 2016. He has served as an Editor for nine international journals, including the IEEE TRANSACTIONS ON WIRELESS COMMUNICATIONS from 2007 to 2009, the IEEE TRANSACTIONS ON VEHICULAR TECHNOLOGY since 2011, and the IEEE TRANSACTIONS ON COMMUNICATIONS since 2015. He was the lead Guest Editor for the IEEE JOURNAL ON SELECTED AREAS IN COMMUNICATIONS, Special Issue on Vehicular Communications and Networks. He was also a Guest Editor for the IEEE JOURNAL ON SELECTED AREAS IN COMMUNICATIONS, Special Issue on Spectrum and Energy Efficient Design of Wireless Communication Networks and Special Issue on Airborne Communication Networks, and a Guest Editor for the IEEE TRANSACTIONS ON BIG DATA, Special Issue on Wireless Big Data.

Xiaodong Wang (S'98–M'98–SM'04–F'08) received the Ph.D. degree in electrical engineering from Princeton University. He is currently a Professor of Electrical Engineering with Columbia University, New York, NY, USA.

His research interests include the general areas of computing, signal processing, and communications. He has published extensively in these areas. Among his publications is a book *Wireless Communication Systems: Advanced Techniques for Signal Reception*, (Prentice Hall in 2003). His current research interests include wireless communications, statistical signal processing, and genomic signal processing.

Dr. Wang received the 1999 NSF CAREER Award, the 2001 IEEE Communications Society and the Information Theory Society Joint Paper Award, and the 2011 IEEE Communication Society Award for Outstanding Paper on New Communication Topics. He has served as an Associate Editor for the IEEE TRANSACTIONS ON COMMUNICATIONS, the IEEE TRANSACTIONS ON WIRELESS COMMUNICATIONS, the IEEE TRANSACTIONS ON SIGNAL PROCESSING, and the IEEE TRANSACTIONS ON INFORMATION THEORY. He listed as an ISI Highly-cited Author.

Fangjiong Chen (M'06) received the B.S. degree in electronics and information technology from Zhejiang University, Hangzhou China, in 1997, and the Ph.D. degree in communication and information engineering from the South China University of Technology, Guangzhou China, in 2002. He joined the School of Electronics and Information Engineering, South China University of Technology. He was a Lecturer from 2002 to 2005 and an Associate Professor from 2005 to 2011.

He is currently a Full-Time Professor with the School of Electronics and Information Engineering, South China University of Technology. He is also the Director of the Department of Underwater Detection and Imaging, Mobile Ultrasonic Detection National Research Center of Engineering Technology. His research interests include signal detection and estimation, array signal processing, and wireless communication.

Prof. Chen received the National Science Fund for Outstanding Young Scientists in 2013.He was elected in the New Century Excellent Talent Program of MOE, China, in 2012.

Jie Tang (S'10–M'13–SM'18) received the B.Eng. degree in information engineering from the South China University of Technology, Guangzhou, China, in 2008, the M.Sc. degree (Hons.) in communication systems and signal processing from the University of Bristol, U.K., in 2009, and the Ph.D. degree from Loughborough University, Leicestershire, U.K., in 2012. He held the Postdoctoral research positions with the School of Electrical and Electronic Engineering, University of Manchester, U.K. He is currently an Associate Professor with the School of Electronic and Information Engineering, South China University of Technology, China.

His research interests include green communications, NOMA, 5G networks, SWIPT, heterogeneous networks, cognitive radio and D2D communications. He is currently serving as an Editor for the IEEE ACCESS, *EURASIP Journal on Wireless Communications and Networking*, *Physical Communications*, and *Ad Hoc & Sensor Wireless Networks*. He also served as a track co-chair for the IEEE Vehicular Technology Conference 2018.

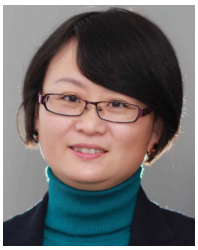

Fei Ji (M'06) received the Ph.D. degree from the South China University of Technology in 1998. She joined the South China University of Technology as a Lecturer. She was an Associate Professor from 2003 to 2008. She was with the City University of Hong Kong, as a Research Assistant, from 2001 to 2002, and a Senior Research Associate from 2005 to 2005. She was with the University of Waterloo, as a Visiting Scholar, from 2009 to 2010. She is currently a Full-Time Professor with the South China University of Technology. Her research interests include wireless communication system and networking.